Differences in the toxin profiles of *Alexandrium ostenfeldii* (Dinophyceae) strains isolated from different geographic origins: Evidence of paralytic toxin, spirolide, and gymnodimine

Pablo Salgado[a,d] , Pilar Riobó[b], Francisco Rodríguez[c], José M. Franco[b], Isabel Bravo[c,*]

[a]Instituto de Fomento Pesquero (IFOP), Enrique Abello 0552, Casilla 101, Punta Arenas, Chile

[b]Instituto de Investigaciones Marinas (IIM-CSIC), Eduardo Cabello 6, 36208, Vigo, Spain

[c]Instituto Español de Oceanografía (IEO), Centro Oceanográfico de Vigo, Subida a Radio Faro 50, 36390, Vigo, Spain

[d]*Present address*: Instituto Español de Oceanografía (IEO), Centro Oceanográfico de Vigo, Subida a Radio Faro 50, 36390, Vigo, Spain

* Corresponding author. E-mail address: isabel.bravo@vi.ieo.es

Abstract

Among toxin-producing dinoflagellates of the genus *Alexandrium*, *A. ostenfeldii* is the only species able to produce paralytic shellfish poisoning (PSP) toxins, spirolides (SPXs) and gymnodimines (GYMs). In this study we characterized and compared three *A. ostenfeldii* strains isolated from the Baltic, Mediterranean, and southern Chile Seas with respect to their toxin profiles, morphology, and phylogeny. Toxin analyses by HPLC-FD and LC-HRMS revealed differences in the toxin profiles of the three strains. The PSP toxin profiles of the southern Chile and Baltic strains were largely the same and included gonyautoxin (GTX)-3, GTX-2, and saxitoxin (STX), although the total PSP toxin content of the Chilean strain (105.83 ± 72.15 pg cell^{-1}) was much higher than that of the Baltic strain (4.04 ± 1.93 pg cell^{-1}). However, the Baltic strain was the only strain that expressed detectable amounts of analogues of GYM-A and GYM-B/-C (48.27 ± 26.12 pg GYM-A equivalents cell^{-1}). The only toxin expressed by the Mediterranean strain was 13-desmethyl SPX-C (13dMeC; 2.85 ± 4.76 pg cell^{-1}). Phylogenetic analysis based on the LSU rRNA showed that the studied strains belonged to distinct molecular clades. The toxin profiles determined in this study provide further evidence of the taxonomic complexity of this species.

Key words: *Alexandrium ostenfeldii*, toxin profile, paralytic toxin, spirolide, gymnodimine

1. Introduction

The frequency of harmful algal blooms (HABs) produced by marine dinoflagellates has increased worldwide over the last several decades, with serious negative impacts on public health and on the economies of the affected areas (Hallegraeff, 2010). The genus *Alexandrium* is one of the most important genera among HAB species because of its toxicity and cosmopolitan distribution in the coastal environments of sub-arctic, temperate, and tropical zones (Anderson et al., 2012). Unlike other species of *Alexandrium*, and most toxin-producing microalgae, which produce only a single type of toxin, *A. ostenfeldii* produces toxins of two different groups: paralytic or saxitoxins (STXs) and cyclic imines of the spirolide (SPX) and gymnodimine (GYM) type (Hansen et al., 1992; Cembella et al., 2000; Van Wagoner et al., 2011). Of these, STXs and their analogues are the most significant because they are responsible for outbreaks of paralytic shellfish poisoning (PSP), which pose a serious risk for environmental and human health (Hallegraeff, 1993). Although SPXs and GYMs have yet to be linked directly to human intoxications (Richard et al., 2001), these fast-acting toxins induce the rapid death (within minutes) in laboratory mice injected intraperitoneally with toxic methanolic extracts from shellfish contaminated with those lipophilic toxins (Marrouchi et al., 2010; Otero et al., 2011). SPXs, and GYMs are commonly co-extracted with other lipophilic toxins, such as the diarrheic toxins okadaic acid and its analogues, which are produced by several *Dinophysis* and *Prorocentrum* species. Thus, in HAB monitoring programs, the presence of SPXs and GYMs in shellfish samples can produce false-positives in mouse bioassay tests for the detection of diarrheic shellfish poisoning toxins (Biré et al., 2002).

SPXs were first isolated and characterized from shellfish collected along the southeastern coast of Nova Scotia, Canada (Hu et al., 1995). Subsequently, *A. ostenfeldii* was identified as the producer of these toxins (Cembella et al., 2000). However, some strains of *A. ostenfeldii*, from diverse geographic regions, also produce PSP toxins (Hansen et al., 1992; MacKenzie et al., 1996; Lim et al., 2005; Kremp et al., 2009; Borkman et al., 2012; Gu et al., 2013) (see Table 1 for additional references). Moreover, this species was recently confirmed to produce GYMs, which block acetylcholine receptors (Kharrat et al., 2008) and are associated with neurotoxic shellfish poisoning. The only other producer of GYMs identified to date is the phylogenetically distant dinoflagellate *Karenia selliformis* (Haywood et al., 2004). GYM-A was initially isolated and characterized in the early 1990s from New Zealand oysters (MacKenzie, 1994; Seki et al., 1995). Later, two additional isomeric analogues (GYM-B and GYM-C) were isolated from cultures of *K. selliformis* (Miles et al., 2000, 2003). GYMs were detected for the first time in a dinoflagellate genus other than *K. selliformis* in an isolate of *A. peruvianum* from North Carolina (USA), in which a novel GYM congener (12-methylgymnodimine, 12MeGYM) was identified (Van Wagoner et al., 2011). This was followed by a report of acyl ester derivatives of GYMs in Tunisian clams (De la Iglesia et al., 2012).

The difficulties in distinguishing the geographic boundaries of *A. ostenfeldii* and the morphologically very similar and also toxic *A. peruvianum* have complicated attempts to define the toxin profiles of these species. According to Balech (1995) *A. ostenfeldii* differs from *A. peruvianum* mainly in the shape of the first apical (1′), and the anterior (s.a.), and posterior (s.p.) sulcal plates. However, plate morphology is highly variable within populations from the same

94 geographic area and even within strains (Lim et al., 2005; Kremp et al., 2009;
95 Kremp et al., 2014), resulting in a great deal of confusion in assigning
96 specimens to one species or the other (Kremp et al., 2009). In fact, recent
97 phylogenetic analysis from cultures characterized as *A. ostenfeldii* or *A.*
98 *peruvianum* based on morphological characters identified six distinct but closely
99 related groups, although these characters were highly variable and not
100 consistently distributed among the groups (Kremp et al., 2014). This
101 demonstrated the invalid initial separation of the two species and led those
102 authors to propose the discontinuation of *A. peruvianum* as a species and its
103 consideration as synonymous with *A. ostenfeldii*, at least until additional data
104 become available.

105 In this study, we used toxin profiles and morphological and molecular taxonomy
106 to characterize three *A. ostenfeldii* strains isolated from three different
107 geographic origins, the Baltic, Mediterranean, and Chilean Southern Seas. To
108 facilitate comparisons of these strains with those from other regions, the
109 literature information on *A. ostenfeldii* toxin profiles worldwide is summarized in
110 Table 1.

111

112 **2. Material and Methods**

113 *2.1. Strains and culture conditions*

114 Cultures were established from three non-clonal strains of *A. ostenfeldii* (or its
115 synonymous *A. peruvianum*) maintained in the culture collection of toxic
116 microalgae of the Spanish Institute of Oceanography in Vigo (CCVIEO:

117 http://www.vgohab.es/). The three strains, from three distantly separated
118 geographic origins, were: 1) the Baltic Sea strain AOTV-B4A (Åland, Finland),
119 2) the Mediterranean Sea strain VGO956 (Palamós, Spain), and 3) the southern
120 Chilean strain AOA32-2 (Vergara Island, Aysén, Chile). These three strains can
121 be considered as geographically representative of each region based on
122 literature data and on our own preliminary study. Specifically, the Baltic and
123 Mediterranean Sea strains were described in Kremp et al. (2009) and Franco et
124 al. (2006), respectively, showing the consistency of their toxin profiles with
125 those of other strains from the respective region. For the Chilean strain, our
126 preliminary analyses carried out with three strains (AOIVAY, AOA32-1, and
127 AOA32-2) from Aysén showed that their toxin profiles were identical, although
128 with different total PSP toxin contents (estimations in early stationary phase of
129 21.1, 33.5, and 16.2 pg cell^{-1}, respectively) in the same experimental conditions
130 (salinity of 32, 15 ºC). The strain AOA32-2 was chosen because it presented
131 the best physiological state, reaching in early stationary phase higher cell
132 concentrations than the other two strains.

133 The strains (starting density 500–800 cell mL^{-1}) were cultured in 100-mL
134 Erlenmeyer flasks filled with 75 mL of L1 medium without silica (Guillard and
135 Hargraves, 1993) and incubated with a photon flux density of 80–100 μmol m^{-2}
136 s^{-1} and a photoperiod of 12:12 h light:dark. Different temperatures and salinities
137 were settled for each strain (Table 2). The medium was prepared using
138 seawater collected from the Galician continental shelf at a depth of 5 m and
139 adjusted to the salinities listed in Table 2 by the addition of sterile MQ water
140 (Milli-Q; Millipore, USA). The cultures were acclimated gradually to the different
141 salinities (max. 3–4 salinity units at a time) and temperatures for at least three

142 transfers after reaching the early stationary phase. A 66-mL sample was taken
143 from each of the 27 cultures during the exponential growth phase and used as
144 follows: 60 mL were processed for toxin analyses (PSP toxin and cyclic imines),
145 3 mL were fixed with Lugol for cell measurements and counts, and 3 mL were
146 fixed with formaldehyde for morphological studies. Additionally, a 1.5-mL
147 sample was processed from three cultures (one culture of each strain, chosen
148 randomly) for molecular analysis, thereby obtaining a total sample volume of
149 67.5 mL from these cultures.

150

151 *2.2. Morphological characterization*

152 Morphological studies, including examination of the plates of the cultured cells
153 by Calcofluor white staining (Flourescent Brightner 28, Sigma) (Fritz and
154 Triemer (1985), were performed using a Leica DMLA microscope (Leica
155 Microsystems, Wetzlar, Germany) equipped with UV epifluorescence and an
156 AxioCam HRc camera (Zeiss, Göttingen, Germany). Species identification and
157 morphological comparisons among the three studied strains were based on the
158 original descriptions and on more recent ones (Balech and de Mendiola, 1977;
159 Balech and Tangen, 1985; Balech, 1995).

160 The lengths and widths of 30 randomly selected cells were measured at 630 X
161 magnification using an Axiocam HRC digital camera (Zeiss, Germany)
162 connected to a Leica DMLA light microscope. Mean cell biovolume (v) was
163 calculated by assuming that the cells were prolate spheroids (Sun and Liu
164 (2003) and using the following equation:

$$v = \frac{\pi}{6} \cdot b^2 \cdot a$$

where a is the cell length and b is the cell width. The statistical analyses were performed using SPSS v.21 software. One-way ANOVA followed by Tukey's post-hoc test was used to identify significant differences in morphometric measurements between strains and treatments.

2.3. Toxin extraction

Toxin analyses were performed on exponentially growing cultures. A Lugol-fixed aliquot was collected from each flask to determine cell density by light microscopy using a Sedgewick–Rafter chamber. Two 30-mL culture subsamples were filtered through GF/F glass-fiber filters (25 mm diameter) (Whatman, Maidstone, England) and kept at –20 °C. Once removed from the freezer, followed by sonication (1 min, 50 Watts) and two rounds of centrifugation (14,000 rpm, 10 min, 5 °C), one of the filters was extracted twice with 0.05 M acetic acid for PSP toxin analysis and the other with 100% methanol for SPX and GYM toxin analyses. The extracts (1.5 mL) were kept at –20 °C until used in the respective analyses, at which time acetic extracts were thawed and methanolic extracts were tempered to be subsequently filtered through 0.45-μm syringe filters.

2.4. Analysis of PSP toxins

PSP toxins were analyzed by high-performance liquid chromatography (HPLC) with post-column oxidation and fluorescence detection (FD) according to the method of Rourke et al. (2008) with slight modifications using a Zorbax Bonus RP column (4.6 × 150 mm, 3.5 μm). The analyses were carried out using a Waters Acquity ultra performance liquid chromatography (UPLC) system (Waters, USA). Mobile phase A was composed of 11 mM heptane sulfonate in a 5.5 mM phosphoric acid aqueous solution adjusted to pH 7.1 with ammonium hydroxide. Mobile phase B consisted of 88.5% 11 mM heptane sulfonate in a 16.5 mM phosphoric acid aqueous solution adjusted to pH 7.1 with ammonium hydroxide and 11.5% acetonitrile. The mobiles phases were filtered through a 0.2-μm membrane before use. A gradient was run at a flow rate of 0.8 mL min^{-1} starting at 100% A and held for 8 min. Mobile phase B was then increased linearly to 100% in 8 min. The gradient was kept at 100% B for 9 min and then returned in 0.1 min to 100% A. An equilibration time of 5 min was allowed prior to the next injection. The total duration of the run was 30 min. The eluate from the column was mixed continuously with 7 mM periodic acid in 50 mM potassium phosphate buffer (pH 9.0) at a rate of 0.4 mL min^{-1} and was heated at 65 °C by passage through a coil of Teflon tubing (0.25 mm i.d., 8 m long). It was then mixed with 0.5 M acetic acid at 0.4 mL min^{-1} and pumped by a two-pump Waters Reagent Manager into the fluorescence detector, which was operated at an excitation wavelength of 330 nm. Emission at 390 nm was recorded. Data acquisition and data processing were performed using the Empower data system (Waters). Toxin concentrations were calculated from calibration curves obtained for the peak area and amount of each toxin. Injection volumes of 20 μL were used for each extract. Standards for the PSP

toxins gonyautoxin (GTX)-4, GTX-1, dcGTX-3, dcGTX-2, GTX-3, GTX-2, neoSTX, dcSTX, and STX were acquired from the NRC Certified Reference Materials program (Halifax, NS, Canada). To verify the presence of, GTX-6 and GTX-5, the samples were boiled with an equal volume of 0.4 M HCl for 15 min to hydrolyze the sulfonic group of the N-sulfocarbamoyl, yielding the corresponding carbamoyl toxins (Franco and Fernandez Vila, 1993).

2.5. Analyses of lipophilic toxins (SPXs and GYMs)

SPX and GYM toxins were identified by liquid chromatography coupled to high-resolution mass spectrometry (LC–HRMS). Samples in methanol were analyzed on a Dionex Ultimate 3000 LC system (Thermo Fisher Scientific, San Jose, California) coupled to an Exactive mass spectrometer (Thermo Fisher Scientific, Bremen, Germany) equipped with an Orbitrap mass analyzer and a heated electrospray source (H–ESI II). Nitrogen (purity > 99.999%) was used as the sheath gas, auxiliary gas, and collision gas. The instrument was calibrated daily in positive and negative ion modes. Mass acquisition was performed in positive ion mode without and with all ion fragmentation (AIF) with a high-energy collisional dissociation (HCD) of 45 eV. The mass range was *m/z* 100–1000 in both full-scan and AIF modes.

SPXs and GYMs were separated and quantified according to the Standardized Operating Procedure (SOP) validated by the European Union Reference Laboratory for Marine Biotoxins (EURLMB, 2011). The X-Bridge C18 column (100 × 2.1 mm, 2.5 μm) was maintained at 25 °C; the injection volume was 20 μL and the flow rate 400 μL min^{-1}. Mobile phase A consisted of water, and

234 mobile phase B of acetonitrile/water (95:5 v/v), both containing 2 mM
235 ammonium formate and 50 mM formic acid. Linear gradient elution started at
236 10% B, increasing to 80% B in 4 min, where it was held for 2 min before the
237 initial conditions of 10% B were restored in 0.5 min; the latter condition was
238 maintained for 2.5 min to allow column equilibration. The total duration of the
239 run was 9 min. Cyclic imines were identified by comparing their retention times
240 with those of the available standards. The peaks in the chromatogram were
241 identified by the exact masses of the diagnostic, fragment, and isotope ions.
242 Cyclic imine standards for 13-desmethyl SPX-C (13dMeC; CRM-SPX-1 7.06 ±
243 0.4 μg mL^{-1}) and GYM-A (CRM-GYM-A 5 ± 0.2 μg mL^{-1}) were acquired from
244 the NRC Certified Reference Materials program (Halifax, NS, Canada). In case
245 another SPX or GYM different from the standards was identified in samples,
246 they were quantified as 13dMeC or GYM-A equivalents, based on the
247 respective calibrations available and assuming equal responses.

248

249 *2.6. DNA extraction, PCR amplification, and sequencing*

250 Exponentially growing vegetative cells from strains AOTV-B4A, VGO956, and
251 AOA32-2 were harvested from the respective 1.5-mL subsamples by
252 centrifugation (13,000 rpm for 2 min) in 1.5-mL Eppendorf tubes. The cells were
253 washed with sterile MQ water, centrifuged as described above, and the
254 resulting pellet was stored overnight at –80 °C. The next day, the samples were
255 thawed, treated with 100 μL of 10% Chelex 100 beads (BioRad, Hercules, CA,
256 USA), placed in a 95 °C Eppendorf Mastercycler EP5345 thermocycler
257 (Eppendorf, New York, USA) for 10 min, and then vortexed. The boiling and

vortex steps were repeated, after which the samples were centrifuged (13,000 rpm for 1 min) and the supernatants subsequently transferred to clean 200-μL tubes, avoiding carryover of the Chelex beads. The samples were kept at −20°C until needed.

Polymerase chain reaction (PCR) amplification of the D1/D2 domains of the large subunit (LSU) rRNA gene was performed using the primer pair D1R/D2C (5'-ACCCGCTGAATTTAAGCATA-3'/5'-ACGAACGATTTGCACGTCAG-3') (Lenaers et al., 1989). The 25-μL amplification reaction mixtures contained 2.5 μL of reaction buffer, 2 mM $MgCl_2$, 0.25 pmol of each primer, 2 mM of dNTPs, 0.65 units of Taq DNA polymerase (Qiagen, CA, USA), and 1 μL of the Chelex extracts. The DNA was amplified in an Eppendorf Mastercycler EP5345 under the following conditions: initial denaturation at 95 °C for 1 min, followed by 40 cycles of denaturation at 54 °C for 1 min, annealing at 72 °C for 3 min, extension at 72 °C for 3 min, and a final extension at 72 °C for 10 min. A 10-μL aliquot of each PCR was checked by agarose gel electrophoresis (1% TAE, 50 V) and SYBR Safe DNA gel staining (Invitrogen, CA, USA).

The PCR products were purified with ExoSAP–IT (USB, Cleveland, OH, USA). The purified DNA was sequenced using the Big Dye Terminator v3.1 reaction cycle sequencing kit (Applied Biosystems, Foster City, CA, USA) and separated on an AB 3130 sequencer (Applied Biosystems) at the CACTI sequencing facilities (Universidade de Vigo, Spain). The LSU sequences obtained in this study for strains AOTV-B4A and VGO956 were deposited in the GenBank database (Acc. Nos. KP782039 and KP782040, respectively). The LSU sequence for Chilean strain AOA32-2 (Acc. No. KF479200) was deposited in

Genbank during a Chilean study carried out in parallel to this one (G. Pizarro, IFOP, personal comm.). The sequences of the studied strains were compared with 40 sequences of other *A. ostenfeldii*/*peruvianum* strains obtained from Genbank. *A. insuetum* and *A. minutum* sequences were used as outgroups to root the tree.

The LSU sequences were aligned using BioEdit v.7.2.5. The final alignment for the LSU phylogeny consisted of 543 positions. The phylogenetic model was selected using MEGA 6 software. A Tamura's 3-parameter model (Tamura, 1992) with a gamma-shaped parameter (γ = 0.213) was selected. The phylogenetic relationships were determined using the maximum likelihood (ML) method of MEGA 6 and the Bayesian inference method (BI) with a general time reversible model from Mr.Bayes v3.1 (Huelsenbeck and Ronquist, 2001). The reconstructed topologies were very similar with the two methods. The phylogenetic tree was represented using the ML results, with bootstrap values from the ML method (*n* = 1000 replicates) and posterior probabilities from the BI method.

3. Results

3.1. Morphology of the organisms

Microscopic examination of the plate morphologies of cultured cells from the Baltic Sea (AOTV-B4A) and the Chilean Southern Sea (AOA32-2) generally agreed well with the original description of *A. ostenfeldii* by Balech and Tangen (1985), and those of the Mediterranean Sea strain (VGO956) with the original

description of *A. peruvianum* by Balech and de Mendiola (1977). A detailed analysis of the thecal plates showed that most of the specimens of the three strains had a narrow and elongated 1′ plate with a prominent ventral pore located on its anterior right side. These plates terminated with a pointed or flat margin that made contact with the s.a. plate (Fig. 1A, B, E, J). However, other 1′ plate features were also observed, mainly in strains VGO956 and AOA32-2. In VGO956, two other types of 1′ plates were seen: one with a less elongated shape and a widely opened ventral pore (Fig. 1F) and another with a rhomboid shape and large enclosed ventral pore (Fig. 1G). Strain AOA32-2 (southern Chile) also exhibited another different elongated 1′ plate (Fig. 1K) with straight margins and an elliptical ventral pore.

The s.a. plate in strain VGO956 was almost always triangular (Fig. 1E), but door-latch-shaped plates were also seen. Both shapes were also characteristic of the s.a. plates of strains AOTV-B4A and AOA32-2 but door-latch-shaped plates were more common (Fig. 1B, J, N). In the Chilean strain (AOA32-2), an additional s.a. plate type, with a shape intermediated between the door-latch and triangular shapes, was also detected (Fig. 1M). Finally, the s.p. plates of all strains were highly variable in shape and not all of them had a connection pore (Fig. 1C, D, H, I, O, P).

The cells occurred as solitary individuals in most cultures, but chains of two cells were observed occasionally. In general, the cells were round to ellipsoidal in shape, with a cell biovolume ranging from 3691 μm^3 (equivalent to 20.63 μm long and 18.49 μm wide) to 104746 μm^3 (61.03 μm long and 57.26 μm wide) (Fig. 2A). The largest cells were generally more ellipsoidal in shape than the

329 smaller cells, which were round. The sizes of the cells differed significantly
330 among the three strains (ANOVA: $P < 0.05$; $n = 270$), with cells of strain
331 AOA32-2 being significantly ($P < 0.001$) the largest and those of strain VGO956
332 the smallest (Fig. 2A). The 95% mean confidence intervals (95% CIs) for the
333 cell lengths and widths of the three strains were: 38.40 ± 0.89 μm and 34.97 ±
334 0.72 μm for strain AOTV-B4A; 31.53 ± 0.68 μm and 29.07 ± 0.62 μm for strain
335 VGO956, and 43.22 ± 0.80 μm and 40.05 ± 0.64 μm for strain AOA32-2.
336 Although cultures of all three strains consisted of both large and small cells, the
337 largest size ranges occurred in strains AOTV-B4A and AOA32-2 (Fig. 2B–D).
338 The size range also varied depending on the temperature and salinity, besides
339 the intrinsic characteristics of the strains. For example, as shown in Fig. 2B,
340 when strain AOTV-B4A was incubated at 19 °C, the cell size ranges observed
341 at salinities of 18 and 25 differed significantly (cell length: mean ± SD of 33.88 ±
342 3.25 μm and 42.89 ± 9.98 μm, respectively; $P < 0.05$; $n = 30$). Growth at the
343 lowest temperatures resulted in significantly ($P < 0.05$; $n = 90$) larger cells for all
344 three strains (Fig. 2B–D), with those of strain AOA32-2 incubated at a salinity of
345 32 (Fig. 2D) having the highest mean cell biovolume (95% CIs for a mean
346 length and width: 51.94 ± 2.32 μm and 46.96 ± 1.82 μm).

347

348 *3.2. Phylogeny*

349 The three selected strains from the three distant geographic regions grouped in
350 different clades (Fig. 3). In the LSU rDNA phylogeny, Baltic strain AOTV-B4A
351 grouped together with other *A. ostenfeldii* strains from the Baltic Sea (Finland,
352 Sweden, Poland, and Denmark), New River and Narragansett (USA), and Bohai

353 Sea (China). These sequences constituted a clade with low support (BI 0.51).
354 Strain VGO956 grouped with its sister strains (IEOVGOAMD12 and
355 IEOVGOAM10C) from the Spanish Mediterranean Sea, near Palamós, but also
356 with North Sea strains from Fal River (UK) and Lough Swilly (Ireland) in a well-
357 supported monophyletic clade (ML 99%, BI 1.0). Strain AOA32-2, from southern
358 Chile, emerged in a separate branch (ML 70%, BI 0.93) together with a strain
359 (IMPLBA033) from Callao (Peru).

360

361 *3.3. PSP toxins*

362 LC analyses showed detectable amounts of PSP toxins in all of the cultures of
363 Baltic and Chilean strains (AOTV-B4A and AOA32-2, respectively), but not in
364 the Mediterranean strain (VGO956). The toxin profiles of the two PSP-toxin-
365 producing strains were the same (Fig. 4), although the toxin content of the
366 Chilean strain (mean ± SD of 105.83 ± 72.15 pg cell^{-1}) was much higher than
367 that of the Baltic strain (mean ± SD of 4.04 ± 1.93 pg cell^{-1}), which is according
368 to the observed differences in their cell sizes (biovolume in Table 3, Figs. 2 and
369 5A). Toxin contents and cellular biovolume values for both strains in all of
370 culture conditions are specified in Table 3. Differences in toxin content in
371 relation to temperatures and salinities as well as cell sizes were assessed in
372 Chilean strain AOA32-2; the small amounts of toxin content in AOTV-B4A did
373 not allow that estimation. A significant correlation between toxin content and
374 biovolume was observed for Chilean strain (R = 0.96, P < 0.01). Toxin values
375 were highest when the strain was cultured at lower temperatures (10 °C) (mean
376 ± SD of 174.47 ± 91.62 pg cell^{-1}) coinciding with the highest values of biovolume

(Table 3). Lowest toxin contents (around 40–50 pg cell^{-1}) also agreed with the smallest cells and were detected in several temperatures and salinities.

The principal compounds produced by strains AOTV-B4A and AOA32-2 under all experimental conditions were GTX-3, GTX-2, and STX (Fig. 4). However, the toxin profiles of both strains also included trace amounts of dcSTX toxins in all treatments, except two, in which the levels of the latter toxin were undetectable: strain AOTV-B4A at 26 °C and a salinity of 25 and strain AOA32-2 at 10 °C and a salinity of 32. In the latter case, this was the condition in which cell biovolume and PSP toxin content were highest (Fig. 5A and Table 3). The toxin profile of strain AOTV-B4A was dominated by GTX-3 (81.9%), followed by STX (14.7%), GTX-2 (3%), and trace amounts (<0.5%) of dcSTX. The toxin profile of strain AOA32-2 was very similar to that of strain AOTV-B4A: GTX-3 (88.2%), STX (7.6%), GTX-2 (3.8%), and dcSTX (<0.5%). These proportions were mostly unchanged when the strains were cultured at different temperatures and salinities.

3.4. Cyclic imine toxins

LC–HRMS analyses of the organic extracts from the cultures showed that only strain VGO956 produced SPXs. Extracts of this Mediterranean strain contained 13dMeC at a retention time (RT) = 8.832 min. 13dMeC yielded a protonated molecule at *m*/*z* 692.4522 $[M+H]^+$. The fragment ions generated in the HCD cell from the peak of 13dMeC were: the loss of a water molecule at *m*/*z* 674.4415 $[C_{42}H_{60}NO_6]^+$, *m*/*z* 444.3108 $[C_{27}H_{42}NO_4]^+$, *m/z* 342.2796 $[C_{23}H_{36}NO]^+$, *m*/*z* 230.1904 $[C_{16}H_{24}N]^+$, *m*/*z* 220.2062 $[C_{15}H_{26}N]^+$, *m*/*z* 206.1906 $[C_{14}H_{24}N]^+$, *m*/*z*

204.1749 $[C_{14}H_{22}N]^+$, *m*/*z* 177.1513 $[C_{12}H_{19}N]^+$, and *m*/*z* 164.1435 $[C_{11}H_{18}N]^+$. The fragment ion at *m*/*z* 164.1435 was the most intense and characteristic. In addition to 13dMeC, others SPXs were screened [20MeG, A, B, C, and D, desmethyl SPX-D, and the unknown SPXs listed in Sleno et al. (2004)], but they were not detected in any of the samples.

On a per cell basis, content of 13dMeC increased with increasing salinity and temperature. The highest contents were recorded at 26 °C (Fig. 5B and Table 3). At temperatures of 15 °C and 19 °C, the toxin content ranged from 0.004 pg $cell^{-1}$ to 0.58 pg $cell^{-1}$, with the lowest content measured in cells grown at 15 °C and a salinity of 14 (Fig. 5B and Table 3). No correlation between SPX content and cell size was observed.

GYM content by the three strains was also analyzed using LC–HRMS. New GYM compounds were observed only in Baltic strain AOTV-B4A, GYM-B/-C analogues (Fig. 6A, B) and a new analogue of GYM-A (Fig. 6C, D). The latter compound was probably a positional isomer based on its mass and fragmentation spectrum (Table 4). The RT of this unknown GYM-A analogue was 4.27 min, which differed by 0.71 min from the RT of the GYM-A standard 3.56 min (Fig. 6E, F). To verify that the difference in the RT was not due to the sample matrix, one sample extract of AOTV-B4A was spiked with GYM-A standard. The RT of GYM-A was not altered by a matrix effect. Their mass spectra were qualitatively the same, including HCD fragment ions, but the percentages of the fragments differed (Fig. 6B, D). Thus, in the mass spectrum of the GYM-A standard (Fig. 6F) the abundance of the fragment $[M+H-H_2O]^+$ at *m*/z 490.3312 was more intense than that by the protonated molecule at *m*/*z*

508.3418 $[M+H]^+$, while the opposite was true for the GYM-A analogue (Fig. 6D). Characteristic HCD fragment ions of GYM-A were also detected in the GYM-A analogue (Table 4). In our search for GYM-B/-C toxins, a chromatogram for the mass range *m/z* 524–525 was acquired for the extract prepared from strain AOTV-B4A. It showed one peak at a RT of 4.01 min (Fig. 6A), which differed by +0.45 min from the RT of GYM-A (Fig. 6E, F). GYM-B/-C standards were not available to confirm the identity of these analogues in our samples but based on their more polar chemical structure, characterized by an additional exocyclic methylene at C17 and a hydroxyl group at C-18 (Miles et al., 2000, 2003), a shorter retention than that of GYM-A (RT 3.56 min) (Fig. 6E, F) in a reverse phase column (Marrouchi et al., 2010) was expected. The compound eluted at RT 4.01 min and produced by strain AOTV-B4 is probably a more lipophilic analogue of GYM-B/-C.

As there are, as yet, no standards for GYM-B and GYM-C and detailed descriptions of their fragmentation patterns have been published, we confirmed these compounds as follows. The accurate mass for the $[M+H]^+$ ion *m/z* 524.3365 $[C_{32}H_{46}NO_5]^+$ with 10.5 relative double bond (RDB) equivalents and -1.049 Δppm was observed. The mass spectral characterization from the AIF experiment for this GYM-B/-C analogue is shown in Table 5. It was compared with the HCD mass spectrum of GYM-B/-C detailed by De la Iglesia et al. (2012). Three characteristic water losses from the protonated molecule, at *m/z* 506.3257, *m/z* 488.3147, and *m/z* 470.3039, were observed. Moreover, a series of common ions with GYM-A as the parent compound were generated in the HCD cell (Table 5).

All samples were also screened for the presence of 12MeGYM but this compound was not detected under any conditions. The highest content of GYMs (113.44 pg GYM-A equivalents $cell^{-1}$) was measured in cells cultured at the highest temperature and salinity (26 °C, salinity of 25). These were also the largest cells (biovolume in Fig. 5B). However, the lowest content of GYMs (around 30–40 pg GYM-A equivalents $cell^{-1}$) were in cells cultured under several intermediate experimental conditions (19 °C, salinity of 18).

4. Discussion

4.1. The detected toxins and their relevance

Toxins from the STX group, SPXs, and GYMs were found in *A. ostenfeldii* (Syn. *A. peruvianum*) in the present study, although their distributions differed in the three studied strains from different geographic locations. Mediterranean strain (VGO956) produced SPXs but not PSP toxins, in agreement with the findings in the literature for *A. ostenfeldii* and *A. peruvianum* strains of the same region (Ciminiello et al., 2006; Franco et al., 2006; Ciminiello et al., 2007; Ciminiello et al., 2010; Riobó et al., 2013; Kremp et al., 2014). The Baltic Sea strain (AOTV-B4A) produced PSP toxins but not SPXs, consistent with the results from other strains from that region (Hakanen et al., 2012; Suikkanen et al., 2013; Kremp et al., 2014). Finally, Chilean strain (AOA32-2) produced only PSP toxins. While this finding is in agreement with that of Pizarro et al. (2012), it contradicts those reported by Almandoz et al. (2014) for *A. ostenfeldii* strains isolated from the Argentinean part of the Beagle Channel (1000 km south of the area where our Chilean strain was isolated), which produced only SPXs (13dMeC and 20MeG).

Among all the toxins detected in *A. ostenfeldii*, those of the STX group are the most dangerous because they may result in the severe and occasionally fatal illness known as PSP syndrome. The threat of PSP syndrome is not only a major cause of concern for public health but is also detrimental to the economy (Anderson et al., 2012). Outbreaks of PSP toxins often result in the death of marine life and livestock and the closure of contaminated fisheries. Together with the continual expenditures required for the maintenance and running of monitoring programs, the economic burden of PSP syndrome is of worldwide significance. Regarding these toxins, it is worth highlight the high PSP toxin content (max. 279.77 pg cell^{-1}) measured in *A. ostenfeldii* cultures from Aysén suggested that this species may be more toxic than previously thought. This conclusion is supported by the environmental conditions in the fjords and channels of Patagonia, where the temperature and salinity (10 ºC and 32, respectively; see Molinet et al., 2003; Almandoz et al., 2014) can be easily the same as those that resulted in the highest cell biovolume and toxin content for this strain in our study (Table 3).

The other two (SPXs and GYMs), belonging to the cyclic imines group have not been directly linked to human intoxications (Richard et al., 2001; Molgó et al., 2014). Currently, there is still a lack of information on the chronic toxicity of cyclic imines or their possible synergy with other toxins that may be present in the same samples. Thus, no regulatory controls have been established for these toxins. The toxicological relevance of this group of toxins and its implication for the safety of shellfish production are not yet completely clear.

The European Food Safety Authority has therefore requested more exposure data to properly assess the risk posed by cyclic imines to shellfish consumers.

4.2. New GYM compounds in A. ostenfeldii

The detection of new GYM compounds in the *A. ostenfeldii* strain from the Baltic Sea, analyzed in this work, provides further insights into both the toxin profile of this specie and scientific knowledge about the GYM complex. As we noted in the Results section, peaks distinct from those of the GYM-A standard appeared in the chromatogram with the same spectrum as GYM-A, although with RTs indicative of their more lipophilic nature. A similar profile was observed by Naila et al. (2012) in clams from the Gulf of Gabes (Tunisia), related to blooms of *K. selliformis*. The authors hypothesized that it was a new isomer of GYM-A or a derivative or weakly bonded aggregate that releases free GYM-A in the ion source. Later, De la Iglesia et al. (2012) confirmed the presence in those samples of gymnodimine fatty acid ester metabolites produced by shellfish. Our search for these compounds in the Baltic strain was, as expected, negative. Harju et al. (2014) found related analogues of GYM-A, B, and C in some Baltic strains. The analogue of GYM-A detected in that study was more lipophilic than the GYM-A standard, as was the derivative present in the Baltic strain from the present work. Therefore, we suspect that these GYM-A analogues are the same compound although we do not have the detailed mass spectrum of their compound to compare with ours. Regarding the GYM-B/-C analogue detected in the present work, it was more lipophilic than GYM-A and therefore also more lipophilic than GYM-B/-C. However, this analogue seems to be different from the two related GYM-B/-C compounds discovered by Harju et al. (2014), since

both are less lipophilic than the GYM-B/-C standard, according to the information on their RTs provided by the authors.

4.3. Differences on the toxin profiles of A. ostenfeldii

The information summarized in Table 1 shows the great variation in the toxin profiles of *A. ostenfeldii* (Syn. *A. peruvianum*) strains from all of the geographic regions where this species and its toxins have been reported. Comparisons of the toxin profiles of these strains are difficult because many of the respective studies do not report all of the toxin groups (PSP toxins and the cyclic imines SPXs and GYMs). In addition, for most of the regions information is still scarce. Nonetheless, valuable information is obtained by preliminary comparisons of the differences in the PSP toxins and/or SPX from different geographic zones. Thus, in the case of the North Atlantic, Baltic Sea, and Mediterranean Sea strains, the PSP/SPX profiles are highly consistent (Fig. 7, see references in Table 1): 1) North Atlantic and Mediterranean Sea strains are mostly characterized by SPX; 2) the Baltic Sea strain is defined by PSP toxin; and 3) the Kattegat Sea strain produces SPX toxins. The latter region can be viewed as a transitional one between the Baltic Sea and the North Sea (Hansen et al., 1992). For the Chilean strains, our data showed an invariable toxin profile characterized only by PSP toxins, although more data are required from Aysén and other nearby areas to confirm the distribution and variability of *A. ostenfeldii*'s toxin profiles in the region.

An important question is whether toxin profiles change in response to changing environmental conditions. In the present study, the strains steadily produced the

same types of toxins (PSP toxins, SPXs, and GYMs) independent of the experimental temperature and salinity conditions. Rather, these variables affected only cell growth and the quantity of the PSP toxins, although the order of dominance (GTX-3, STX, and GTX-2) was preserved. The same has been reported in other studies showing that the production of either SPXs or PSP toxins was not induced by changes in salinity, temperature, or CO_2 supply, which instead affected the relative content of the different PSP toxins and SPX analogues (Otero et al., 2010; Kremp et al., 2012; Suikkanen et al., 2013). Similar effects have been reported for nutrients and growth phase in *A. ostenfeldii* cultures (Anderson et al., 1990; Hwang and Lu, 2000; Granéli and Flynn, 2006; Hu et al., 2006). In the case of GYMs, the scarce data prevent any conclusions on the consistency of the appearance of these toxins and the variations related to the physicochemical conditions of the cultures. We found much higher content of GYMs (maximum of 113.44 pg GYM-A equivalents $cell^{-1}$ vs. a minimum of 27.77 pg GYM-A equivalents $cell^{-1}$) under the highest temperature and salinity (26 °C, salinity of 25) conditions than under other conditions.

4.4. Phylogeny and morphology related to strains and their toxin profiles

The results of the phylogenetic analysis showed that the three strains of *A. ostenfeldii* grouped with other strains of different geographic origin and their phylogenetic classification was coincident with previous studies (Kremp et al., 2014; Tillmann et al., 2014). Moreover, the toxin profiles of those groups have common features that merit discussion. According to our LSU analysis, Mediterranean strain (VGO956), with a toxin profile composed solely of

572 13dMeC, was grouped with strains sharing the same toxin profile as those from
573 Fal River (UK), Lough Swilly (Ireland), and Palamós (Mediterranean Spain)
574 (Table 1). Such clade corresponds to the Group 2 of other phylogenetic studies
575 (Kremp et al., 2014; Tillmann et al., 2014). The Chilean strains analyzed in the
576 present study grouped within a phylogenetic clade, a subgroup of Group 6 of
577 Kremp et al. (2014), that includes a Peruvian strain (IMPLBA033), with which
578 they shared the characteristic of producing only PSP toxins (Kremp et al., 2014;
579 Table 1). The only difference in the toxin profiles was that in some cases trace
580 amounts of dcSTX were detected in the Chilean strains (Table 1). Finally, the
581 Baltic Sea strain (AOTV-B4A) formed a monophyletic group with other strains
582 from the same area, as reported by Tahvanainen et al. (2012). The clade also
583 includes strains from the Atlantic coast of the USA (Borkman et al., 2012;
584 Tomas et al., 2012), one Chinese strain (ASBH01) (Gu et al., 2013), and
585 another from eastern Denmark (K1354) (Kremp et al., 2014). All Baltic strains of
586 this monophyletic clade, which correspond to Group 1 of Kremp et al. (2014),
587 are known to produce PSP toxins. The toxin profile of Baltic *A. ostenfeldii* was
588 shown by Kremp et al. (2014) and Suikkanen et al. (2013) to include GTX-3,
589 STX, and GTX-2, which agrees with the results of our study. However, unlike
590 the other strains in the clade, the Chinese strain produces only STX and
591 neoSTX (Gu et al., 2013) and not GTXs. However, all of these Group 1 strains
592 are STX producers (Kremp et al., 2014).

593 With respect to the morphological features of the strains, the Baltic Sea (AOTV-
594 B4A) and Chilean Southern Sea (AOA32-2) strains more closely match the *A.*
595 *ostenfeldii* description of Balech and Tangen (1985), and the Mediterranean
596 Sea strain (VGO956) the *A. peruvianum* description of Balech and de Mendiola

(1977). However, coinciding with Kremp et al. (2014), the morphological study carried out in this work showed a tabulation of the thecal plates too variable to be of use in defining and separating the above mentioned genetically determined groups.

Conclusions

The morphology, phylogeny, and toxin profiles of the three geographically differentiated strains of *A. ostenfeldii* investigated in this study corroborate both the dissimilarities in toxin production and the taxonomic complexities reported in the literature for this species complex. While the Mediterranean Sea strain was characterized by its SPX content, the Chilean strain was defined by PSP toxins and the Baltic Sea strain by PSP toxins and new GYM analogues. The PSP toxin profiles of the southern Chile and Baltic strains were coincident in their inclusion of GTX-3, GTX-2, and STX. However, the Chilean strain was much more toxic than the Baltic strain. The latter was the only strain with detectable amounts of GYM compounds: analogues of GYM-A and GYM-B/-C. The toxin contents (PSP toxins and/or SPX) of the three strains coincide with those of other strains already reported from the same geographic origin and belonging to the same phylogenetic group. This provides support for the recognition of PSP toxins and/or SPX production as a characteristic phenotypic trait of the genetically isolated populations, as already suggested in the literature. However, in the case of GYM compounds, further studies are needed before any related, definitive conclusions can be reached.

621 **Acknowledgments**

622 The authors express their gratitude to A. Kremp for kindly giving strain AOTV-
623 B4A to CCVIEO. We thank P.A. Díaz for help with R plotting, M. García for
624 support in the phylogeny, A. Fernández-Villamarín for technical assistance in
625 processing the toxin samples, and I. Ramilo and P. Rial for technical assistance
626 with the cultures. This work is a contribution of Unidad Asociada “Microalgas
627 Nocivas” (CSIC-IEO) and was carried out at the Instituto Español de
628 Oceanografía (IEO) in Vigo and was financially supported by the CCVIEO
629 project and CICAN-2013-40671-R (Ministry of Economy and Competitiveness).
630 P. Salgado is a researcher at the IFOP, which provides financial support for his
631 doctoral staying.

632

633 **References**

634

635 Aasen, J., MacKinnon, S., LeBlanc, P., Walter, J., Hovgaard, P., Aune, T.,
636 Quilliam, M., 2005. Detection and Identification of Spirolides in Norwegian
637 Shellfish and Plankton. Chem. Res. Toxicol. 18, 509–515.

638 Almandoz, G., Montoya, N., Hernando, M., Benavides, H., Carignan, M.,
639 Ferrario, M., 2014. Toxic strains of the *Alexandrium ostenfeldii* complex in
640 southern South America (Beagle Channel, Argentina). Harmful Algae 37, 100–
641 109.

642 Amzil, Z., Sibat, M., Royer, R., Masson, N., Abadie, E., 2007. Report on the
643 First Detection of Pectenotoxin-2, Spirolide-A and Their Derivatives in French
644 Shellfish. Marine Drugs 5, 168–179.

645 Anderson, D.M., Alpermann, T., Cembella, A., Collos, Y., Masseret, E.,
646 Montresor, M., 2012. The globally distributed genus *Alexandrium*: Multifaceted
647 roles in marine ecosystems and impacts on human health. Harmful Algae 14,
648 10–35.
649 Anderson, D.M., Kulis, D.M., Sullivan, J.J., Hall, S., 1990. Toxin composition
650 variations in one isolate of the dinoflagellate *Alexandrium fundyense*. Toxicon
651 28, 885–893.
652 Balech, E., 1995. The Genus *Alexandrium* Halim (Dinoflagellata). Sherkin Island
653 Marine Station, Sherkin Island Co., Cork, Ireland.
654 Balech, E., de Mendiola, B.R., 1977. Un nuevo *Gonyaulax* productor de
655 hemotalasia en Perú. Neotropica 23, 49–54.
656 Balech, E., Tangen, K., 1985. Morphology and taxonomy of toxic species in the
657 tamaresis group (Dinophyceae): *Alexandrium excavatum* (Braarud) comb. nov.
658 and *Alexandrium ostenfeldii* (Paulsen) comb. nov. Sarsia 70, 333–343.
659 Beuzenberg, V., Mountfort, D., Holland, P., Shi, F., MacKenzie, L., 2012.
660 Optimization of growth and production of toxins by three dinoflagellates in
661 photobioreactor cultures. J. Appl. Phycol. 24, 1023–1033.
662 Biré, R., Krys, S., Frémy, J.M., Dragacci, S., Stirling, D., Kharrat, R., 2002. First
663 evidence on occurrence of gymnodimine in clams from Tunisia. J. Nat. Toxins
664 11, 269–275.
665 Borkman, D., Smayda, T., Tomas, C., York, R., Strangman, S., Wright, J., 2012.
666 Toxic *Alexandrium peruvianum* (Balech and de Mendiola) Balech and Tangen in
667 Narragansett Bay, Rhode Island (USA). Harmful Algae 19, 92–100.

668 Brown, L., Bresnan, E., Graham, J., Lacaze, J.P., Turrell, E., Collins, C., 2010.
669 Distribution, diversity and toxin composition of the genus *Alexandrium*
670 (Dinophyceae) in Scottish waters. Eur. J. Phycol. 45, 375–393.
671 Burson, A., Matthijs, H., de Bruijne, W., Talens, R., Hoogenboom, R., Gerssen,
672 A., Visser, P., Stomp, M., Steur, K., van Scheppingen, Y., Huisman, J., 2014.
673 Termination of a toxic *Alexandrium* bloom with hydrogen peroxide. Harmful
674 Algae 31, 125–135.
675 Cembella, A., Bauder, A., Lewis, N., Quilliam, M., 2001. Association of the
676 gonyaulacoid dinoflagellate *Alexandrium ostenfeldii* with spirolide toxins in size-
677 fractionated plankton. J. Plankton Res. 23, 1413–1419.
678 Cembella, A., Lewis, N., Quilliam, M., 2000. The marine dinoflagellate
679 *Alexandrium ostenfeldii* (Dinophyceae) as the causative organism of spirolide
680 shellfish toxins. Phycologia 39, 67–74.
681 Ciminiello, P., Dell'Aversano, C., Dello Iacovo, E., Fattorusso, E., Forino, M.,
682 Grauso, L., Tartaglione, L., Guerrini, F., Pezzolesi, L., Pistocchi, R., 2010.
683 Characterization of 27-hydroxy-13-desmethyl spirolide C and 27-oxo-13,19-
684 didesmethyl spirolide C. Further insights into the complex Adriatic *Alexandrium*
685 *ostenfeldii* toxin profile. Toxicon 56, 1327–1333.
686 Ciminiello, P., Dell'Aversano, C., Fattorusso, E., Forino, M., Grauso, L.,
687 Tartaglione, L., Guerrini, F., Pistocchi, R., 2007. Spirolide Toxin Profile of
688 Adriatic *Alexandrium ostenfeldii* Cultures and Structure Elucidation of 27-
689 Hydroxy-13,19-didesmethyl Spirolide C. J. Nat. Prod. 70, 1878–1883.
690 Ciminiello, P., Dell'Aversano, C., Fattorusso, E., Magno, S., Tartaglione, L.,
691 Cangini, M., Pompei, M., Guerrini, F., Boni, L., Pistocchi, R., 2006. Toxin profile

692 of *Alexandrium ostenfeldii* (Dinophyceae) from the Northern Adriatic Sea
693 revealed by liquid chromatography–mass spectrometry. Toxicon 47, 597–604.
694 De la Iglesia, P., McCarron, P., Diogène, J., Quilliam, M.A., 2012. Discovery of
695 gymnodimine fatty acid ester metabolites in shellfish using liquid
696 chromatography/mass spectrometry. Rapid Commun. Mass Spectrom. 27, 643–
697 653.
698 EURLMB, 2011. EU-Harmonised Standard Operating Procedure for
699 Determination of Lipophilic Marine Biotoxins in Molluscs by LC–MS/MS.
700 European Union Reference Laboratory for Marine Biotoxins.
701 http://aesan.msps.es/en/CRLMB/web/home.shtml.
702 Franco, J.M., Fernandez Vila, P., 1993. Separation of paralytic shellfish toxins
703 by reversed phase high performance liquid chromatography with postcolumn
704 reaction and fluorimetric detection. Cromatographia 35, 613–620.
705 Franco, J.M., Paz, B., Riobó, P., Pizarro, G., Figueroa, R., Fraga, S., Bravo, I.,
706 2006. First report of the production of spirolids by *Alexandrium peruvianum*
707 (Dinophyceae) from the Mediterranean Sea, 12th International Conference on
708 Harmful Algae, Copenhagen, Denmark, 4–8 September.
709 Fritz, L., Triemer, R.E., 1985. A rapid simple technique utilizing Calcoflour White
710 M2R for the visualization of dinoflagellate thecal plates. J. Phycol. 21, 662–664.
711 Granéli, E., Flynn, K., 2006. Chemical and physical factors influencing toxin
712 content, in: Granéli, E., Turner, J. (Eds.), Ecology of Harmful Algae, ed.
713 Ecological Studies Series 189., Springer-Verlag Berlin Heidelberg.
714 Gribble, K., Keafer, B., Quilliam, M., Cembella, A., Kulis, D., Manahan, A.,
715 Anderson, D.M., 2005. Distribution and toxicity of *Alexandrium ostenfeldii*
716 (Dinophyceae) in the Gulf of Maine, USA. Deep-Sea Res. Pt. II 52, 2745–2763.

717 Gu, H., Zeng, N., Liu, T., Yang, W., Müller, A., Krock, B., 2013. Morphology,
718 toxicity, and phylogeny of *Alexandrium* (Dinophyceae) species along the coast
719 of China. Harmful Algae 27, 68–81.
720 Guillard, R.R.L., Hargraves, P.E., 1993. Stichochrysis immobilis is a diatom, not
721 achrysophyte. Phycologia 32, 234–236.
722 Hakanen, P., Suikkanen, S., Franzén, J., Franze, H., Kankaanpää, H., Kremp,
723 A., 2012. Bloom and toxin dynamics of *Alexandrium ostenfeldii* in a shallow
724 embayment at the SW coast of Finland, northern Baltic Sea. Harmful Algae 15,
725 91–99.
726 Hallegraeff, G.M., 1993. A review of harmful algal blooms and their apparent
727 global increase. Phycologia 32, 79–99.
728 Hallegraeff, G.M., 2010. Ocean climate change, phytoplankton community
729 responses, and harmful algal blooms: a formidable predictive challenge. J.
730 Phycol. 46, 220–235.
731 Hansen, P., Cembella, A., Moestrup, Ø., 1992. The marine dinoflagellate
732 *Alexandrium ostenfeldii*: Paralytic shellfish toxin concentration, composition, and
733 toxicity to a tintinnid ciliate. J. Phycol. 28, 597–603.
734 Harju, K., Kremp, A., Suikkanen, S., Kankaanpää, H., Vanninen, P., 2014. Mass
735 spectrometric screening of novel gymnodimine-like compounds in isolates of
736 *Alexandrium ostenfeldii*, 16th Internation Conference on Harmful Algae,
737 Wellington, New Zealand.
738 Haywood, A., Steidinger, K., Truby, E., Bergquist, P., Bergquist, P., Adamson,
739 J., MacKenzie, L., 2004. Comparative morphology and molecular phylogenetic
740 analysis of three new species of the genus *Karenia* (Dinophyceae) from New
741 Zealand. J. Phycol. 40, 165–179.

742 Hu, T., Chen, W., Shi, Y., Cong, W., 2006. Nitrate and phosphate
743 supplementation to increase toxin production by the marine dinoflagellate
744 *Alexandrium tamarense*. Mar. Pollut. Bull. 52, 756–760.
745 Hu, T., Curtis, J., Oshima, Y., Quilliam, M., Walter, J., Watson-Wright, W.,
746 Wright, J., 1995. Spirolides B and D, two novel macrocycles isolated from the
747 digestive glands of shellfish. J. Chem. Soc., Chem. Commun, 2159–2161.
748 Huelsenbeck, J.P., Ronquist, F., 2001. MrBAYES: Bayesian inference of
749 phylogenetic trees. Bioinformatics 17, 754–755.
750 Hwang, D., Lu, Y., 2000. Infuence of environmental and nutritional factors on
751 growth, toxicity, and toxin profile of dinoflagellate *Alexandrium minutum*.
752 Toxicon 38, 1491–1503.
753 Jester, R., Rhodes, L., Beuzenberg, V., 2009. Uptake of paralytic shellfish
754 poisoning and spirolide toxins by paddle crabs (*Ovalipes catharus*) via a bivalve
755 vector. Harmful Algae 8, 369–376.
756 Kaga, S., Sekiguchi, K., Yoshida, M., Ogata, T., 2006. Occurrence and toxin
757 production *Alexandrium* spp. (Dinophyceae) in coastal waters of Iwate
758 Prefecture, Japan. Nippon Suisan Gakk. 72, 1068–1076.
759 Katikou, P., Aligizaki, K., Zacharaki, T., Iossifidis, D., Nikolaidis, G., 2010. First
760 report of spirolides in Greek shellfish associated with causative *Alexandrium*
761 species, 14th International Conference on Harmful Algae, Crete, Greek, 1–5
762 November.
763 Kharrat, R., Servent, D., Girard, E., Ouanounou, G., Amar, M., Marrouchi, R.,
764 Benoit, E., Molgó, J., 2008. The marine phycotoxin gymnodimine targets
765 muscular and neuronal nicotinic acetylcholine receptor subtypes with high
766 affinity. J. Neurochem. 107, 952–963.

767 Kremp, A., Godhe, A., Egardt, J., Dupont, S., Suikkanen, S., Casabianca, S.,
768 Penna, A., 2012. Intraspecific variability in the response of bloom-forming
769 marine microalgae to changed climate conditions. Ecol. Evol. 2, 1195–1207.
770 Kremp, A., Lindholm, T., Dreßler, N., Erler, K., Gerdts, G., Eirtovaara, S.,
771 Leskinen, E., 2009. Bloom forming *Alexandrium ostenfeldii* (Dinophyceae) in
772 shallow waters of the Åland Archipelago, Northern Baltic Sea. Harmful Algae,
773 318–328.
774 Kremp, A., Tahvanainen, P., Litaker, W., Krock, B., Suikkanen, S., Leaw, C.P.,
775 Tomas, C., 2014. Phylogenetic relationships, morphological variation, and toxin
776 patterns in the *Alexandrium ostenfeldii* (Dinophyceae) complex: implications for
777 species boundaries and identities. J. Phycol. 50, 81–100.
778 Lenaers, G., Maroteaux, L., Michot, B., Herzog, M., 1989. Dinoflagellates in
779 evolution. A molecular phylogenetic analysis of large subunit ribosomal RNA. J.
780 Mol. Evol. 29, 40—51.
781 Lim, P.T., Ogata, T., 2005. Salinity effect on growth and toxin production of four
782 tropical *Alexandrium* species (Dinophyceae). Harmful Algae 45, 699–710.
783 Lim, P.T., Usup, G., Leaw, C.P., Ogata, T., 2005. First report of *Alexandrium*
784 *taylori* and *Alexandrium peruvianum* (Dinophyceae) in Malaysia waters. Harmful
785 Algae 4, 391–400.
786 MacKenzie, L., 1994. More blooming problems: toxic algae and shellfish
787 biotoxins in the South Island (January–May 1994). Seafood N. Z. 2, 47–52.
788 MacKenzie, L., White, D., Oshima, Y., Kapa, J., 1996. The resting cyst and
789 toxicity of *Alexandium ostenfeldii* (Dinophyceae) in New Zealand. Phycologia
790 35, 148–155.

MacKinnon, S., Walter, J., Quilliam, M., Cembella, A., LeBlanc, P., Burton, I., Hardstaff, W., Lewis, N., 2006. Spirolides Isolated from Danish Strains of the Toxigenic Dinoflagellate *Alexandrium ostenfeldii*. J. Nat. Prod. 69, 983–987.

Maclean, C., Cembella, A., Quilliam, M., 2003. Effects of Light, Salinity and Inorganic Nitrogen on Cell Growth and Spirolide Production in the Marine Dinoflagellate *Alexandrium ostenfeldii* (Paulsen) Balech et Tangen. Bot. Mar. 46, 466–476.

Marrouchi, R., Benoit , E., Kharrat, R., Molgo, J., 2010. Gymnodimines : a family of phycotoxins contaminating shellfish, in: Berbier, J., Benoit, E., Marchot, P., Mattei, C., Servent, D. (Ed.), Advances and new technologies in Toxinology. SFET Editions: Meetings on Toxinology, E-book RT18., pp. 79–83.

Miles, C., Wilkins, A., Stirling, D., MacKenzie, L., 2000. New Analogue of Gymnodimine from a *Gymnodinium* Species. J. Agric. Food Chem. 48, 1373–1376.

Miles, C., Wilkins, A., Stirling, D., MacKenzie, L., 2003. Gymnodimine C, an Isomer of Gymnodimine B, from *Karenia selliformis*. J. Agric. Food Chem. 51, 4838–4840.

Molgó, J., Aráoz, R., Benoit, E., Iorga, B., 2014. Cyclic imine toxins: chemistry, origin, metabolism, pharmacology, toxicology, and detection, in: Botana, L.M. (Ed.), Seafood and Freshwater Toxins. 3rd edition., CRC Press, Boca Raton, pp. 951–989.

Molinet, C., Lafon, A., Lembeye, G., Moreno, C., 2003. Patrones de distribución espacial y temporal de floraciones de *Alexandrium catenella* (Whedon & Kofoid) Balech 1985, en aguas interiores de la Patagonia noroccidental de Chile. Rev. Chil. Hist. Nat. 76, 681–698.

816 Naila, I.B., Hamza, A., Gdoura, R., Diogène, J., de la Iglesia, P., 2012.
817 Prevalence and persistence of gymnodimines in clams from the Gulf of Gabes
818 (Tunisia) studied by mouse bioassay and LC–MS/MS. Harmful Algae 18, 56–
819 64.
820 Otero, A., Alfonso, A., Vieytes, M.R., Cabado, A.G., Vieites, J.M., Botana, L.M.,
821 2010. Effects of environmental regimens on the toxin profile of *Alexandrium*
822 *ostenfeldii*. Environ. Toxicol. Chem. 29, 301–310.
823 Otero, A., Chapela, M.J., Atanassova, M., Vieites, J.M., Cabado, A.G., 2011.
824 Cyclic imines: chemistry and mechanism of action: a review. Chem. Res.
825 Toxicol. 24, 1817–1829.
826 Pizarro, G., Pesse, N., Salgado, P., Alarcón, C., Garrido, C., Guzmán, L., 2012.
827 Determinación de capacidad de adherencia, mecanismos de propagación y
828 métodos de destrucción de *Alexandrium catenella* (célula vegetativa y quiste).
829 Informe Final. Subsecretaría de Pesca y Acuicultura, p. 278.
830 Ravn, H., Schmidt, C., Sten, H., Anthoni, U., Christophersen, C., Nielsen, P.,
831 1995. Elicitation of *Alexandrium ostenfeldii* (Dinophyceae) affects the toxin
832 profile. Comp. Biochem. Physiol. 111C, 405–412.
833 Richard, D., Arsenault, E., Cembella, A., Quilliam, M., 2001. Investigations into
834 the toxicology and pharmacology of spirolides, a novel group of shellfish toxins,
835 in: Hallegraeff, G.M., Blackburn, S.I., Bolch, C.J., Lewis, R.J. (Eds.), Harmful
836 Algal Blooms 2000. Intergovernmental Oceanographic Commission of
837 UNESCO, pp. 383–386.
838 Riobó, P., Rodriguez, F., Garrido, J.L., Franco, J.M., 2013. Toxin profiles of *A.*
839 *ostenfeldii* and *A. peruvianum*. Comparison of two clonal strains with different
840 light tolerance, Marine and Freshwater Toxins Analysis. Fourth Joint

841 Symposium and AOAC Task Force Meeting, Baiona-Pontevedra, Spain, 5–9
842 May.
843 Roach, J., LeBlanc, P., Lewis, N., Munday, R., Quilliam, M., MacKinnon, S.,
844 2009. Characterization of a Dispiroketal Spirolide Subclass from Alexandrium
845 ostenfeldii. J. Nat. Prod. 72, 1237–1240.
846 Rourke, W.A., Murphy, C.J., Pitcher, G., Van de Riet, J.M., Garth Burns, B.,
847 Thomas, K.M., Quilliam, M.A., 2008. Rapid postcolumn methodology for
848 determination of paralytic shellfish toxins in shellfish tissue. J. AOAC Int. 91,
849 589–597.
850 Rundberget, T., Bunæs, J., Selwood, A., Miles, C., 2011. Pinnatoxins and
851 spirolides in Norwegian blue mussels and seawater. Toxicon 58, 700–711.
852 Seki, T., Satake, K., Mackenzie, L., Kaspar, H., Yasumoto, T., 1995.
853 Gymnodimine, a new marine toxin of unprecedented structure isolated from
854 New Zealand Oysters and the dinoflagellate, *Gymnodinium* sp. Tetrahedron
855 Lett. 36, 7093–7096.
856 Sleno, L., Chalmers, M., Volmer, D., 2004. Structural study of spirolide marine
857 toxins by mass spectrometry. Part II. Mass Spectrometric characterization of
858 unknown spirolides and related compounds in a cultured phytoplankton extract.
859 Anal. Bioanal. Chem. 378, 977–986.
860 Suikkanen, S., Kremp, A., Hautala, H., Krock, B., 2013. Paralytic shellfish toxins
861 or spirolides? The role of environmental and genetic factors in toxin production
862 of the *Alexandrium ostenfeldii* complex. Harmful Algae 26, 52–59.
863 Sun, J., Liu, D., 2003. Geometric models for calculating cell biovolume and
864 surface area for phytoplankton. J. Plankton Res. 25, 1331–1346.

865 Tahvanainen, P., Alpermann, T., Figueroa, R., John, U., Hakanen, P., Nagai,
866 S., Blomster, J., Kremp, A., 2012. Patterns of post-glacial genetic differentiation
867 in marginal populations of a marine microalga. PLoS ONE 7, e53602.
868 Tamura, K., 1992. Estimation of the number of nucleotide substitutions when
869 there are strong transition-transversion and G + C-content biases. Mol. Biol.
870 Evol. 9, 678–687.
871 Tillmann, U., Kremp, A., Tahvanainen, P., Krock, B., 2014. Characterization of
872 spirolide producing *Alexandrium ostenfeldii* (Dinophyceae) from the western
873 Arctic. Harmful Algae 39, 259–270.
874 Tomas, C., Van Wagoner, R., Tatters, R., White, K., Hall, S., Wright, J., 2012.
875 *Alexandrium peruvianum* (Balech and Mendiola) Balech and Tangen a new
876 toxic species for coastal North Carolina. Harmful Algae 17, 54–63.
877 Touzet, N., Franco, J.M., Raine, R., 2008. Morphogenetic diversity and biotoxin
878 composition of Alexandrium (dinophyceae) in Irish coastal waters. Harmful
879 Algae 7, 782–797.
880 Touzet, N., Lacaze, J., Maher, M., Turrell, E., Raine, R., 2011. Summer
881 dynamics of *Alexandrium ostenfeldii* (Dinophyceae) and spirolide toxins in Cork
882 Harbour, Ireland. Mar. Ecol. Prog 425, 21–33.
883 Van Wagoner, R., Misner, I., Tomas, C., Wright, J., 2011. Occurrence of 12-
884 methylgymnodimine in a spirolide-producing dinoflagellate *Alexandrium*
885 *peruvianum* and the biogenetic implications. Tetrahedron Lett. 52, 4243–4246.

886

887 **Table 1**. Toxin profiles of *A. ostenfeldii* strains from different geographic origins worldwide
888

			Type of toxins			
Species	Geographical location	Region	PSP*	SPXs**	GYMs***	Reference
A. ostenfeldii	Åland, Finland	(1)	2	ND	NA	Kremp et al. (2009); Suikkanen et al. (2013)
A. ostenfeldii	Åland, Finland	(1)	4	ND	A anal.; B/C anals.	Riobó et al. (2013)
A. ostenfeldii	Gotland, Sweden	(1)	2	ND	NA	Suikkanen et al. (2013); Kremp et al. (2014)
A. ostenfeldii	Hel, Poland	(1)	2	ND	NA	Kremp et al. (2014)
A. ostenfeldii	Öresund, Denmark	(1)	2	ND	NA	Kremp et al. (2014)
A. ostenfeldii	Baltic Sea	(1)	NI	NI	unkn. comps.; A, B/C anals.	Harju et al. (2014)
A. ostenfeldii	Åland, Finland	(1)	3	ND	A, B/C anals.	This study
A. ostenfeldii	Limfjord, Denmark	(2)	6	NA	NA	Hansen et al. (1992)
A. ostenfeldii	Limfjord, Denmark	(2)	12	NA	NA	Ravn et al. (1995)
A. ostenfeldii	Limfjord, Denmark	(2)	NA	G; 13dMeC; 13,19ddMeC	NA	MacKinnon et al. (2006)
A. ostenfeldii	Kattegat Sea, Denmark	(2)	8	13dMeC; 13,19ddMeC	NA	Otero et al. (2010)
A. ostenfeldii	Sognefjord, Norway	(3)	NA	G; 20MeG	NA	Aasen et al. (2005)
A. ostenfeldii	Ouwerkerkse Kreek, Netherland	(3)	2	13dMeC	N/A	Burson et al. (2014)
A. ostenfeldii	Arcachón, French	(3)	NA	A; 13dMeC	ND	Amzil et al. (2007)
A. ostenfeldii	Bantry Bay, Ireland	(3)	ND	C; D	NA	Touzet et al. (2008)
A. peruvianum	Lough Swilly, Ireland	(3)	ND	13dMeC; 13dMeD	NA	Touzet et al. (2008)
A. ostenfeldii	East coast, Scotland	(3)	1	20MeG	NA	Brown et al. (2010)
A. ostenfeldii	Cork Harbour, Ireland	(3)	NA	13dMeC; 20MeG	NA	Touzet et al. (2011)
A. ostenfeldii	Coast, Norway	(3)	NA	G; isoC; 13dMeC; 13,19ddMeC; 20MeG	NA	Rundberget et al. (2011)
A. ostenfeldii	Skagerrak, North Sea	(3)	ND	20MeG; 13dMeC	NA	Suikkanen et al. (2013)
A. ostenfeldii	East coast, Scotland	(3)	ND	20MeG; 13dMeC	NA	Suikkanen et al. (2013)
A. peruvianum	Lough Swilly, Ireland	(3)	ND	13dMeC	NA	Suikkanen et al. (2013); Kremp et al. (2014)
A. ostenfeldii	Fal River, UK	(3)	ND	13dMeC	NA	Kremp et al. (2014)
A. ostenfeldii	Breidafjord, Iceland	(3)	ND	C; G; 13dMeC; 20MeG	NA	Kremp et al. (2014)
A. ostenfeldii	Oslofjord, Norway	(3)	ND	A; 13,19ddMeC	NA	Kremp et al. (2014)
A. ostenfeldii	North Sea, Norway	(3)	ND	20MeG	NA	Kremp et al. (2014)
A. ostenfeldii	North Sea, Scotland	(3)	ND	20MeG	NA	Kremp et al. (2014)
A. ostenfeldii	North Sea, Scotland	(3)	ND	A; 13dMeC; 20MeG	NA	(Kremp et al., 2014)
A. ostenfeldii	W and S coasts, Greenland	(3)	ND	C; H; 13dMeC; 20MeG; 8 unknown SPXs	NA	Tillmann et al. (2014)
A. peruvianum	Palamós, Spain	(4)	ND	B; C; D; 13dMeC; 13dMeD	NA	Franco et al. (2006)
A. ostenfeldii	Northern Adriatic Sea, Italy	(4)	NA	13dMeC; 13,19ddMeC; 27OH13,19ddMeC	NA	Ciminiello et al. (2007)
A. ostenfeldii	Thermaikos Gulf, Greek	(4)	NA	A; 13dMeC	ND	Katikou et al. (2010)
A. ostenfeldii	Northern Adriatic Sea, Italy	(4)	NA	27OH13dMeC; 27oxo13,19ddMeC	NA	Ciminiello et al. (2010)
A. peruvianum	Palamós, Spain	(4)	ND	13dMeC	NA	Riobó et al. (2013); Kremp et al. (2014); This study
A. ostenfeldii	Nova Scotia, Canada	(5)	NA	A; B; C; D; D2; 13dMeC	NA	Cembella et al. (2001)
A. ostenfeldii	Nova Scotia, Canada	(5)	NA	C; C3; 13dMeC; 13dMeD	NA	Maclean et al. (2003)
A. ostenfeldii	Nova Scotia, Canada	(5)	NA	H; I	NA	Roach et al. (2009)

A. ostenfeldii	Gulf of Maine, USA	(5)	ND	A; B; C; C2; D, D2; 13dMeC	NA	Gribble et al. (2005)
A. peruvianum	New River, NC, USA	(5)	NA	D; 13dMeC	12Me	Van Wagoner et al. (2011)
A. peruvianum	Narragansett, RI, USA	(5)	7	13dMeC	12Me	Borkman et al. (2012)
A. peruvianum	New River, NC, USA	(5)	7	D; 13dMeC	NA	Tomas et al. (2012)
A. ostenfeldii	Saanich, Canada	(5)	NI	NI	A	Harju et al. (2014)
A. ostenfeldii	Big Glory Bay, New Zealand (NZ)	(6)	+	D; 13dMeC; 13dMeD	NA	Jester et al. (2009); Beuzenberg et al. (2012)
A. ostenfeldii	Kaitaia and Tahaora; Timaru, NZ	(6)	2; 9	NA	NA	MacKenzie et al. (1996)
A. peruvianum	Samariang River, Malaysia	(7)	11; 5	NA	NA	Lim et al. (2005); Lim and Ogata (2005)
A. ostenfeldii	Toni Bay, Japan	(7)	10	NA	NA	Kaga et al. (2006)
A. ostenfeldii	Bohai Sea, China	(7)	1	ND	NA	Gu et al. (2013)
A. ostenfeldii	Beagle Channel, Argentina	(8)	ND	13dMeC; 20MeG	NA	Almandoz et al. (2014)
A. peruvianum	Callao, Peru	(8)	2	ND	NA	Kremp et al. (2014)
A. ostenfeldii	Vergara Island, Aysén, Chile	(8)	3	ND	ND	This study

*** 1**: STX, neoSTX; **2**: GTX-2/3, STX; **3**: GTX-2/3, STX, dcSTX; **4**: GTX-2/3, STX, dcSTX, neoSTX; **5**: GTX-1/4/6, dcSTX, neoSTX; **6**: GTX-2/3/6, C1/2; **7**: GTX-2/3/5, STX, C1/2; **8**: GTX-1–5, C1/2; **9**: GTX-2/3/5, STX, dcSTX, neoSTX, C2/3; **10**: GTX-1–6, STX, neoSTX; **11**: GTX1/2/4/5/6, STX, dcSTX, neoSTX; **12**: GTX-2–6, STX, neoSTX, C2–4. ** **A**: SPX-A; **B**: SPX-B; **C**: SPX-C; **C2**: SPX-C2; **C3**: SPX-C3; **isoC**: SPX-isoC; **D**: SPX-D; **D2**: SPX-D2; **G**: SPX-G; **H**: SPX-H, **I**: SPX-I; **13dMeC**: 13-desmethyl SPX-C; **13dMeG**: 13-desmethyl SPX-G; **20MeG**: 20-methyl SPX-G; **13,19ddMeC**: 13,19-didesmethyl SPX-C; **27OH13,19ddMeC**: 27-hydroxy-13,19-didesmethyl SPX-C; **27OH13dMeC**: 27-hydroxy-13-desmethyl SPX-C; **27oxo13,19ddMeC**: 27-oxo-13,19-didesmethyl SPX-C. *** **A**: GYM-A; **B/C**: GYM-B/-C; **12Me**: 12-methyl GYM. **ND**: Not detected; **NI**: Not information; **NA**: Not analyzed; **+:** Positive to PSP toxins; **(1)**: Baltic Sea; **(2)**: Kattegat Sea (Limfjord); **(3)**: Northeastern Atlantic Ocean; **(4)**: Mediterranean Sea, **(5)**: Northwest Atlantic Ocean, **(6)**: New Zealand, **(7)**: Western Pacific Ocean, **(8)**: South America.

Table 2. Strains and treatments used in this study. The original name of the species, the strain code, geographic origin, culture origin, group that isolated the strain, salinity and temperature conditions, and number of treatments of each strain are shown.

Species orig. name	Strain	Location	Culture origin	Isolator	Salinities / Temperatures	Treatments (n)
A. ostenfeldii	AOTV-B4A	Åland, Finland	Vegetative cell	A. Kremp	10, 18, 25 / 15, 19, 26	9
A. peruvianum	VGO956	Palamós, Spain	Resting cyst	I. Bravo	14, 25, 37 / 15, 19, 26	9
A. ostenfeldii	AOA32-2	Vergara I., Chile	Resting cyst	P. Salgado	25, 32, 37 / 10, 15, 19	9

900 **Table 3.** Toxins (pg cell^{-1}) and mean of cell biovolume of the *A. ostenfeldii*
901 strains under different salinity and temperature conditions. (ND: Not detected)

902

Strain	Salinity	Temperature ºC	Biovolume (μm^3)	PSP toxins	SPXs	GYMs
AOTV-B4A	10	15	31227	4,926	ND	32,748
AOTV-B4A	18	15	28729	6,975	ND	54,673
AOTV-B4A	25	15	32838	4,953	ND	47,341
AOTV-B4A	10	19	19689	6,140	ND	27,893
AOTV-B4A	18	19	17873	2,314	ND	27,774
AOTV-B4A	25	19	36040	1,001	ND	39,663
AOTV-B4A	10	26	22769	4,111	ND	46,676
AOTV-B4A	18	26	17249	2,476	ND	44,243
AOTV-B4A	25	26	37286	3,442	ND	113,435
VGO956	14	15	21383	ND	0,004	ND
VGO956	25	15	22298	ND	0,167	ND
VGO956	37	15	13943	ND	0,577	ND
VGO956	14	19	11922	ND	0,054	ND
VGO956	25	19	11399	ND	0,370	ND
VGO956	37	19	12503	ND	0,022	ND
VGO956	14	26	13310	ND	2,309	ND
VGO956	25	26	15637	ND	10,033	ND
VGO956	37	26	15273	ND	12,158	ND
AOA32-2	25	10	45077	130,686	ND	ND
AOA32-2	32	10	61979	279,771	ND	ND
AOA32-2	37	10	42645	112,958	ND	ND
AOA32-2	25	15	24368	55,616	ND	ND
AOA32-2	32	15	34137	73,030	ND	ND
AOA32-2	37	15	29645	49,047	ND	ND
AOA32-2	25	19	29837	43,772	ND	ND
AOA32-2	32	19	40116	99,240	ND	ND
AOA32-2	37	19	37955	108,307	ND	ND

903

904

Table 4. HRMS data obtained from the AIF spectra acquired in the mass range *m/z* 100–1000. List of the measured accurate masses (*m/z*) for $[M+H]^+$ and the product ions of GYM-A as recorded by De la Iglesia et al. (2012) (left), the GYM-A standard from this study (middle), and the GYM-A analogue detected in the Baltic strain from this work (right). Retention times, exact mass and assigned formulae with relative double bonds (RDB) equivalents, and mass accuracy measurements (Δ in ppm) are detailed. ND (not detected).

	mass spectrum GYM-A (De la Iglesia et al. 2013)	**mass spectrum GYM-A (standard) RT 3.56 min**	**mass spectrum GYM-A analogue (AOTV-B4A) RT 4.27 min**
m/z	508,3414	508,3418	508,3417
FORMULA	$C_{32}H_{46}NO_4^+$	$C_{32}H_{46}NO_4^+$	$C_{32}H_{46}NO_4^+$
RDB, Δ ppm	NI, -1.4	10.5 , -0.66	10.5, -0.856
m/z	490,3305	490,3312	490,3311
FORMULA	$C_{32}H_{44}NO_3^+$	$C_{32}H_{44}NO_3^+$	$C_{32}H_{44}NO_3^+$
RDB, Δ ppm	NI, -2.2	11.5, -0.756	11.5, -0.960
m/z	446,3408	446,3413	446,3405
FORMULA	$C_{31}H_{44}NO_2^+$	$C_{31}H_{44}NO_2^+$	$C_{31}H_{44}NO_2^+$
RDB, Δ ppm	NI, -2.2	10.5, -0.989	10.5, -2.782
m/z	410,3045	410,3048	410,305
FORMULA	$C_{27}H_{40}NO_2^+$	$C_{27}H_{40}NO_2^+$	$C_{27}H_{40}NO_2^+$
RDB, Δ ppm	NI, -2.1	8.5, -1.355	8.5, -0.868
m/z	392,2939	392,2943	392,2941
FORMULA	$C_{27}H_{38}NO^+$	$C_{27}H_{38}NO^+$	$C_{27}H_{38}NO^+$
RDB, Δ ppm	NI, -2.2	9.5, -1.252	9.5, -1.762
m/z	368,294	ND	368,2583
FORMULA	$C_{24}H_{37}NO^+$	$C_{24}H_{34}NO_2^+$	$C_{24}H_{34}NO_2^+$
RDB, Δ ppm	NI, -2.2	8.5, -4.089	8.5, -0.287
m/z	304,2266	304,2267	304,2254
FORMULA	$C_{19}H_{30}NO_2^+$	$C_{19}H_{30}NO_2^+$	$C_{19}H_{30}NO_2^+$
RDB, Δ ppm	NI, -1.8	5.5, -1.334	5.5, -5.607
m/z	286,2159	286,2163	286,2163
FORMULA	$C_{19}H_{28}NO^+$	$C_{19}H_{28}NO^+$	$C_{19}H_{28}NO^+$
RDB, Δ ppm	NI, -2.4	6.5, -0.842	6.5, -0.842
m/z	246,1847	246,185	246,1848
FORMULA	$C_{16}H_{24}NO^+$	$C_{16}H_{24}NO^+$	$C_{16}H_{24}NO^+$
RDB, Δ ppm	NI, -2.1	5.5, -0.979	5.51, -1.791
m/z	216,1742	216,1745	216,1744
FORMULA	$C_{15}H_{22}N^+$	$C_{15}H_{22}N^+$	$C_{15}H_{22}N^+$
RDB, Δ ppm	NI, -2.1	5.5, -0.815	5.5, -1.278
m/z	202,1586	202,1589	202,1589
FORMULA	$C_{14}H_{20}N^+$	$C_{14}H_{20}N^+$	$C_{14}H_{20}N^+$
RDB, Δ ppm	NI, -2.0	5.5, -1.119	-0,624
m/z	174,1274	174,1276	174,1276
FORMULA	$C_{12}H_{16}N^+$	$C_{12}H_{16}N^+$	$C_{12}H_{16}N^+$
RDB, Δ ppm	NI, -2.0	5.5, -0.724	5.5, -0.724
m/z	162,1274	162,1275	162,1276
FORMULA	$C_{11}H_{26}N^+$	$C_{11}H_{26}N^+$	$C_{11}H_{26}N^+$
RDB, Δ ppm	NI, -2.0	4.5, -1.394	4.5, -0.778
m/z	136,1118	136,1119	136,1119
FORMULA	$C_9H_{14}N^+$	$C_9H_{14}N^+$	$C_9H_{14}N^+$
RDB, Δ ppm	NI, -1.9	3.5, -1.293	3.5, -1.293

Table 5. HRMS data obtained from AIF spectra acquired in the mass range *m/z* 100-1000. List of measured accurate masses (*m/z*) for $[M+H]^+$ and product ions of GYM-B/-C as recorded by De la Iglesia et al. (2012) (left) and the GYM-B/-C analogue detected in the Baltic strain from this work (right). Retention times, exact mass and assigned formulae with relative double bonds (RDB) equivalents, and mass accuracy measurements (Δ in ppm) are detailed. NI (no information).

	mass spectrum GYM-B/-C (De la Iglesia et al. 2013)	**mass spectrum GYM-B/-C analogue (AOTV-B4A) RT 4.01 min**
m/z	524,3365	524,3375
FORMULA	$C_{32}H_{46}NO_5^+$	$C_{32}H_{46}NO_5^+$
RDB, Δ ppm	NI, -1.1	10.5, 1.240
m/z	506,4	506,3257
FORMULA	$C_{32}H_{44}NO_4^+$	$C_{32}H_{44}NO_4^+$
RDB, Δ ppm	NI, NI	11.5, -1.551
m/z	488,4	488,3147
FORMULA	$C_{32}H_{42}NO_3^+$	$C_{32}H_{42}NO_3^+$
RDB, Δ ppm	NI, NI	12.5, -2.5
m/z	NI	470,3039
FORMULA	NI	$C_{32}H_{40}NO_2^+$
RDB, Δ ppm	NI, NI	13.5, -3.096
m/z	462	462,3358
FORMULA	$C_{31}H_{44}NO_2^+$	$C_{31}H_{44}NO_2^+$
RDB, Δ ppm	NI, NI	10.5, -1.852
Product ion spectrum common with GYM-A		
m/z	368,294	368,2569
FORMULA	$C_{24}H_{37}NO^+$	$C_{24}H_{34}NO_2^+$
RDB, Δ ppm	NI, -2.2	8.5, -4.089
m/z	304,2266	304,2266
FORMULA	$C_{19}H_{30}NO_2^+$	$C_{19}H_{30}NO_2^+$
RDB, Δ ppm	NI, -1.8	5.5, -1.662
m/z	286,2159	286,2159
FORMULA	$C_{19}H_{28}NO^+$	$C_{19}H_{28}NO^+$
RDB, Δ ppm	NI, -2.4	6.5, -2.240
m/z	246,1847	246,1848
FORMULA	$C_{16}H_{24}NO^+$	$C_{16}H_{24}NO^+$
RDB, Δ ppm	NI, -2.1	5.5, -1.791
m/z	216,1742	216,1744
FORMULA	$C_{15}H_{22}N^+$	$C_{15}H_{22}N^+$
RDB, Δ ppm	NI, -2.1	5.5, -1.278
m/z	202,1586	202,1588
FORMULA	$C_{14}H_{20}N^+$	$C_{14}H_{20}N^+$
RDB, Δ ppm	NI, -2.0	5.5, -1.119
m/z	174,1274	174,1276
FORMULA	$C_{12}H_{16}N^+$	$C_{12}H_{16}N^+$
RDB, Δ ppm	NI, -2.0	5.5, -0.724
m/z	162,1274	162,1275
FORMULA	$C_{11}H_{26}N^+$	$C_{11}H_{26}N^+$
RDB, Δ ppm	NI, -2.0	4.5, -1.394
m/z	136,1118	136,1119
FORMULA	$C_9H_{14}N^+$	$C_9H_{14}N^+$
RDB, Δ ppm	NI, -1.9	3.5, -1.293

Fig. 1. Light micrographs of calcofluor-stained *A. ostenfeldii* cells from cultures of strains AOTV-B4A (A–D), VGO956 (E–I), and AOA32-2 (J–P). The 1′ plate including a prominent right-sided ventral pore (arrow) and terminated with a pointed (A) or flat (B, E, J, K) margin (black arrowhead indicates different types of margin that made contact with s.a. plate). Different s.a. plates are shown for each strain (A, E, J). Cells from strains VGO956 and AOA32-2 showing different shapes of 1′ (F, G, K) and s.a. (L–N) plates; are also shown, as is the diversity of the s.p. plates (C, D, H, I, O, P) of the three strains (white arrowhead indicates posterior connection pore). Scale bar = 10 μm.

Fig. 2. Box-plots of the total cell biovolume (*n* = 270) of the three *A. ostenfeldii* strains (A) and the cell biovolume of strains AOTV-B4A (B), VGO956 (C), and AOA32-2 (D) exposed to different salinity and temperature conditions (*n* = 30). Salinity values are shown by colored boxes in the chart.

Fig. 3. Phylogenetic relationships among *A. ostenfeldii* strains based on the D1-D2 LSU rDNA sequences obtained in this study and from GenBank. *A. insuetum* and *A. minutum* sequences were used as outgroups. The phylogenetic tree was constructed using the maximum-likelihood method. Numbers at the branches indicate the percentage of bootstrap support (*n* = 1000) and posterior probabilities based on Bayesian inference as a search criterion. Bootstrap values <50% and probabilities <0.5 are denoted by hyphens. Names in bold represent isolates sequenced for this study.

Fig. 4. Liquid chromatography PSP toxin profiles of *A. ostenfeldii* cultivated at a salinity of 25 and a temperature 19 °C. Strains AOTV-B4A (A) and AOA32-2 (B) produce GTX-3 (5), GTX-2 (6), and STX (9). Chromatogram of the standard PSP mixture (C) of GTX-4 (1), GTX-1 (2), dcGTX-3 (3), dcGTX-2 (4), GTX-3 (5), GTX-2 (6), neoSTX (7), dcSTX (8), and STX (9).

Fig. 5. Cell biovolume and toxin content of *A. ostenfeldii* cultures exposed to different salinity and temperature conditions. Total PSP toxin content (A) in cultures of strains AOTV-B4A (gray circle) and AOA32-2 (black circle). Total content of SPXs in cultures of strains VGO956 (gray circle) and GYMs in cultures of strains AOTV-B4A (black circle) (B). Note that the temperature axis is inverted.

Fig. 6. Selected liquid chromatography coupled to high-resolution mass spectrometry chromatograms (left) and mass spectra (right) from positive ionization mode for *A. ostenfeldii* strain AOTV-B4A (A–D) and the GYM-A standard (E, F). *m/z* 524.3365 [M+H]+ for GYM-B/-C analogue (A, B); *m/z* 508.3417 [M+H]+ for GYM-A analogue (C, D).

Fig. 7. Global distribution of PSP toxins, SPXs, and GYMs of *A. ostenfeldii* strains reported in the literature. The figure is based on the studies listed in Table 1, which include analyses of PSP toxins and SPXs performed for the same strains as well as literature data on GYMs.

Figure

Click here to download high resolution image

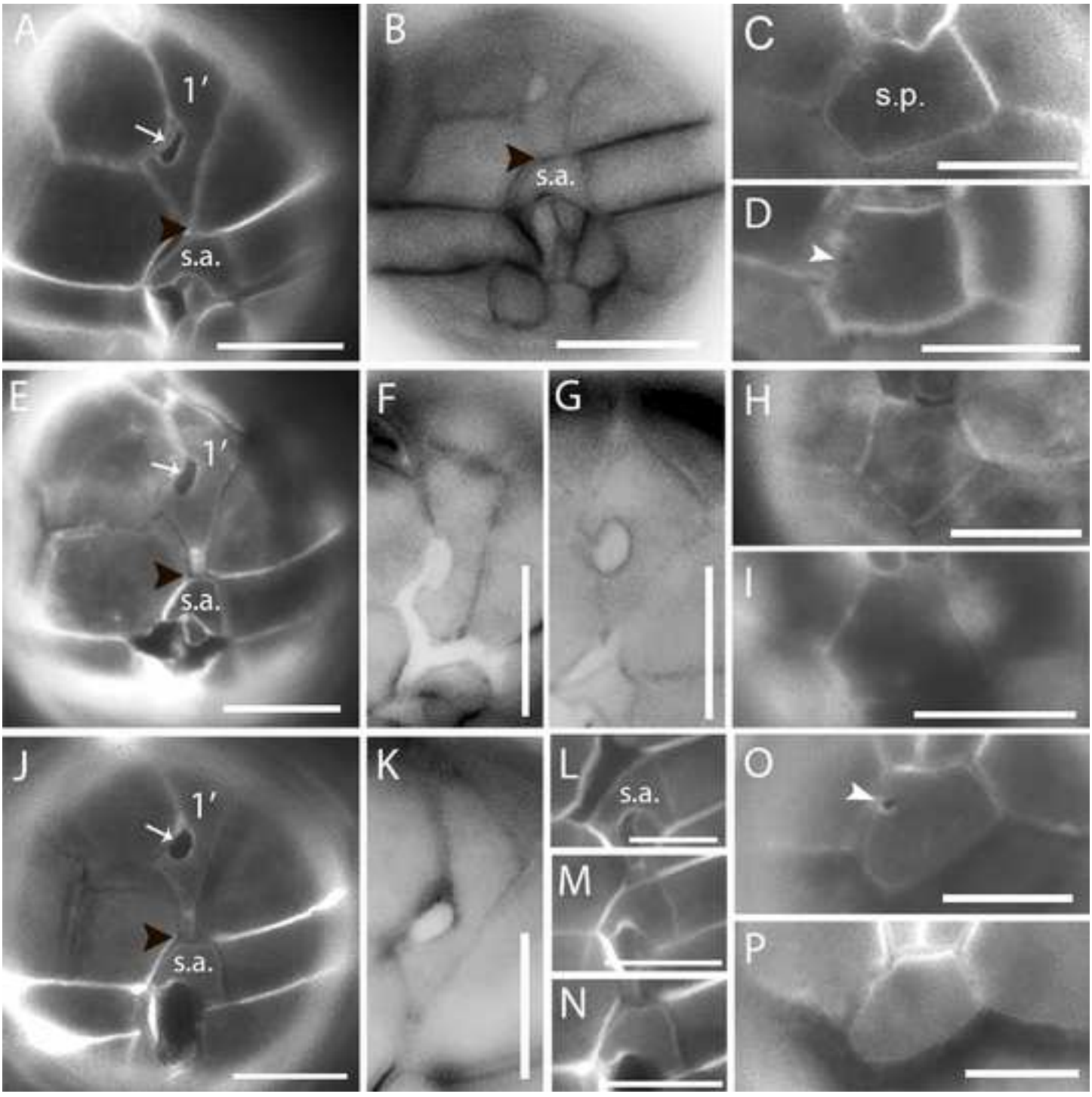

Figure
Click here to download high resolution image

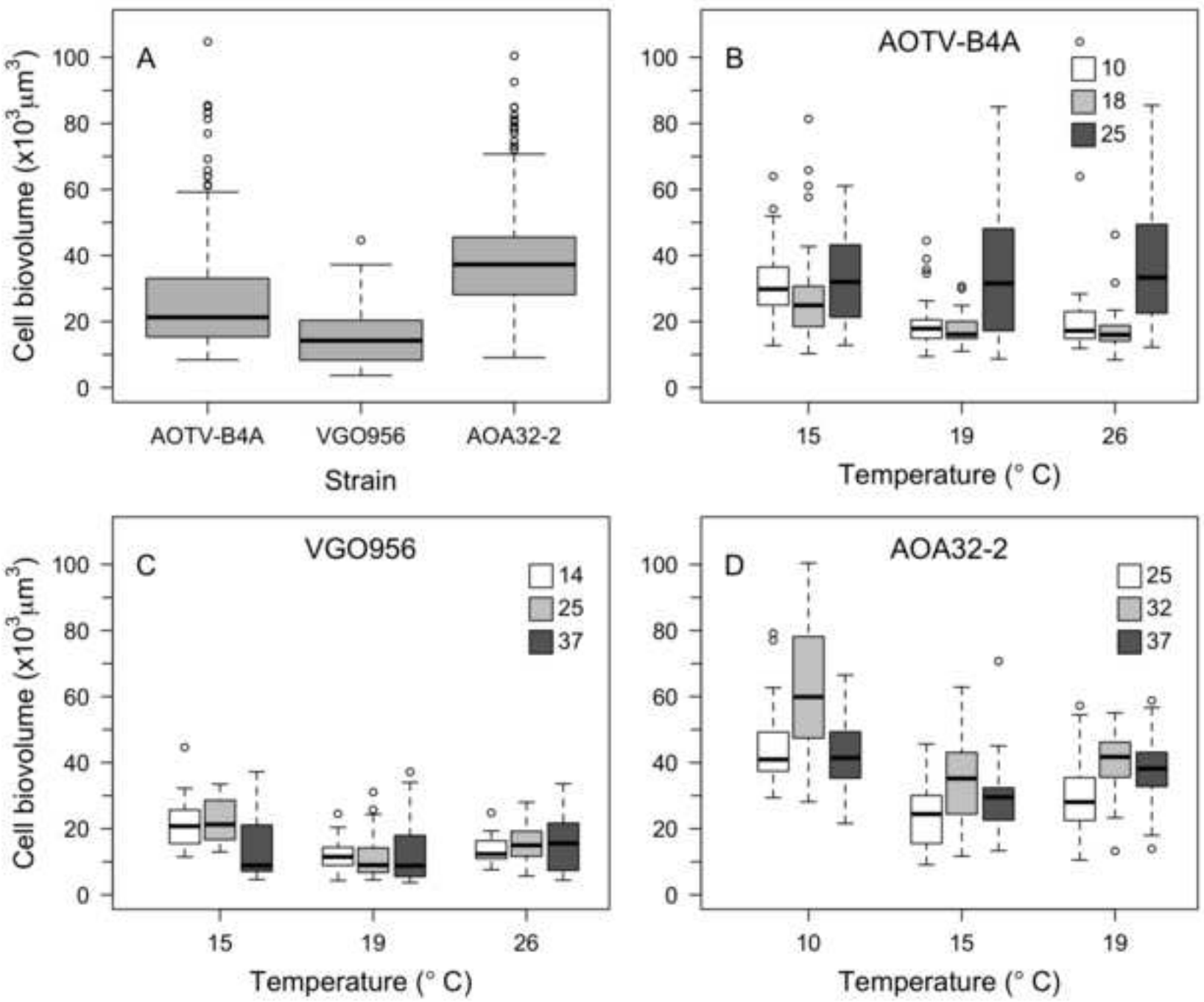

Figure

Click here to download high resolution image

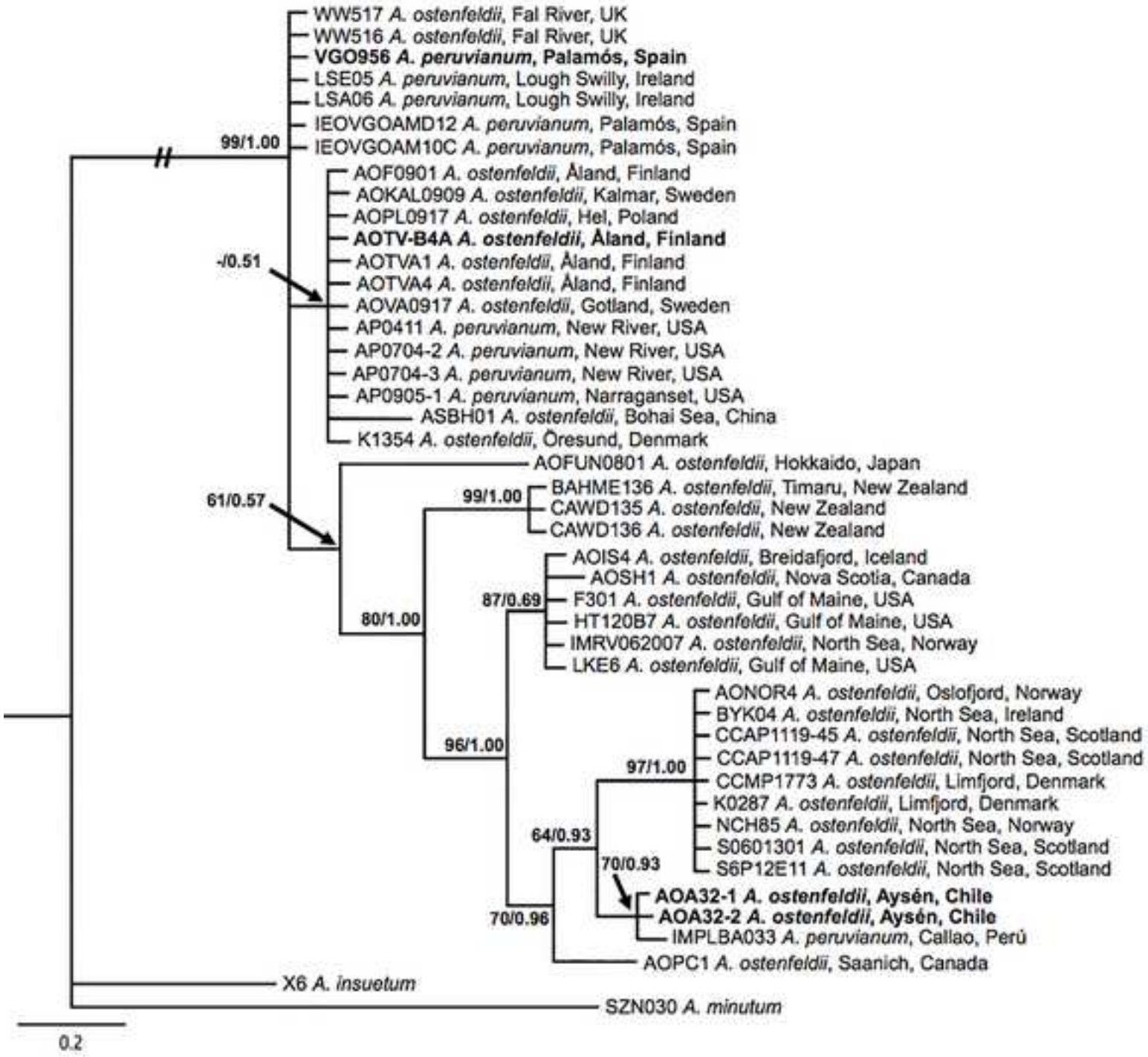

Figure
Click here to download high resolution image

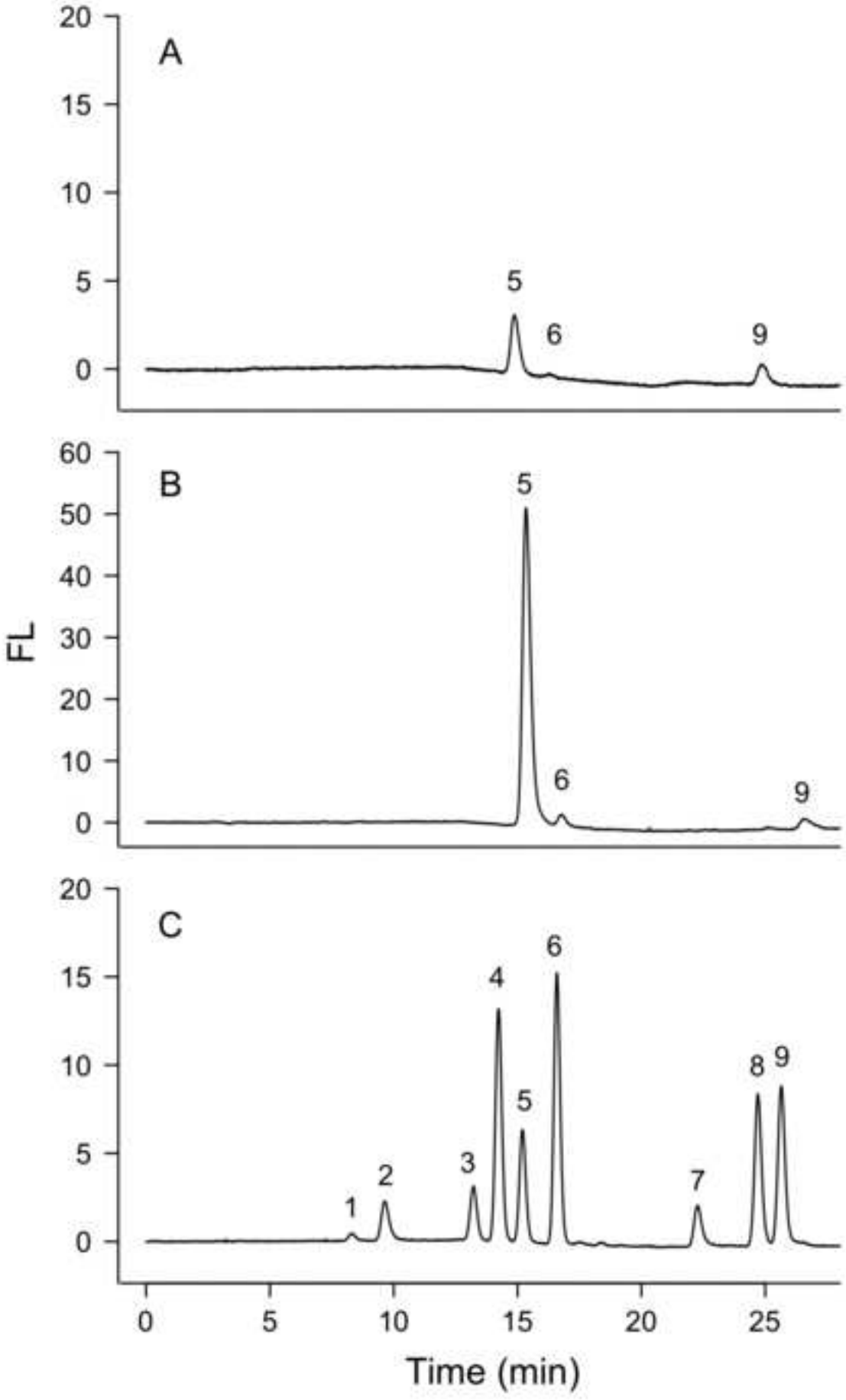

Figure
Click here to download high resolution image

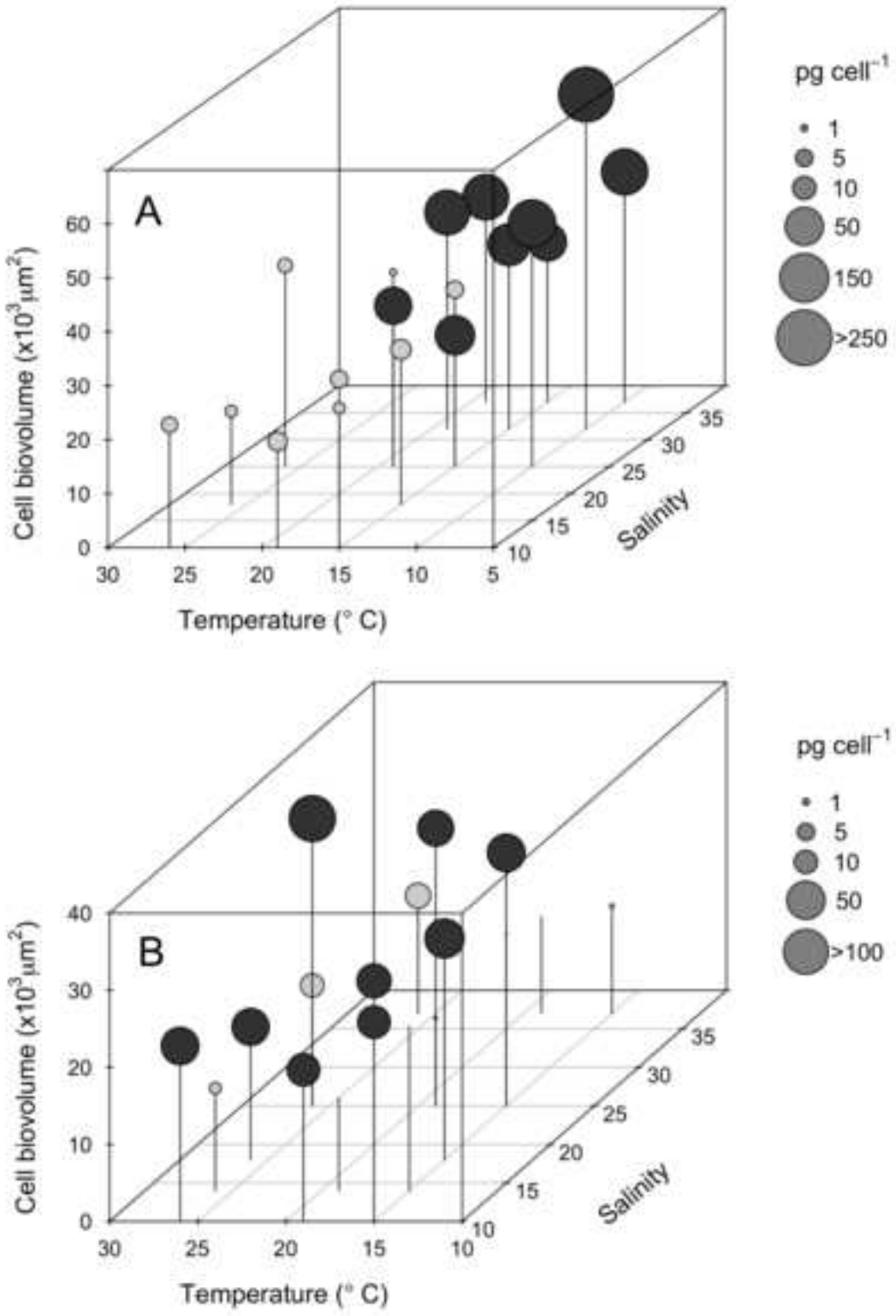

Figure
Click here to download high resolution image

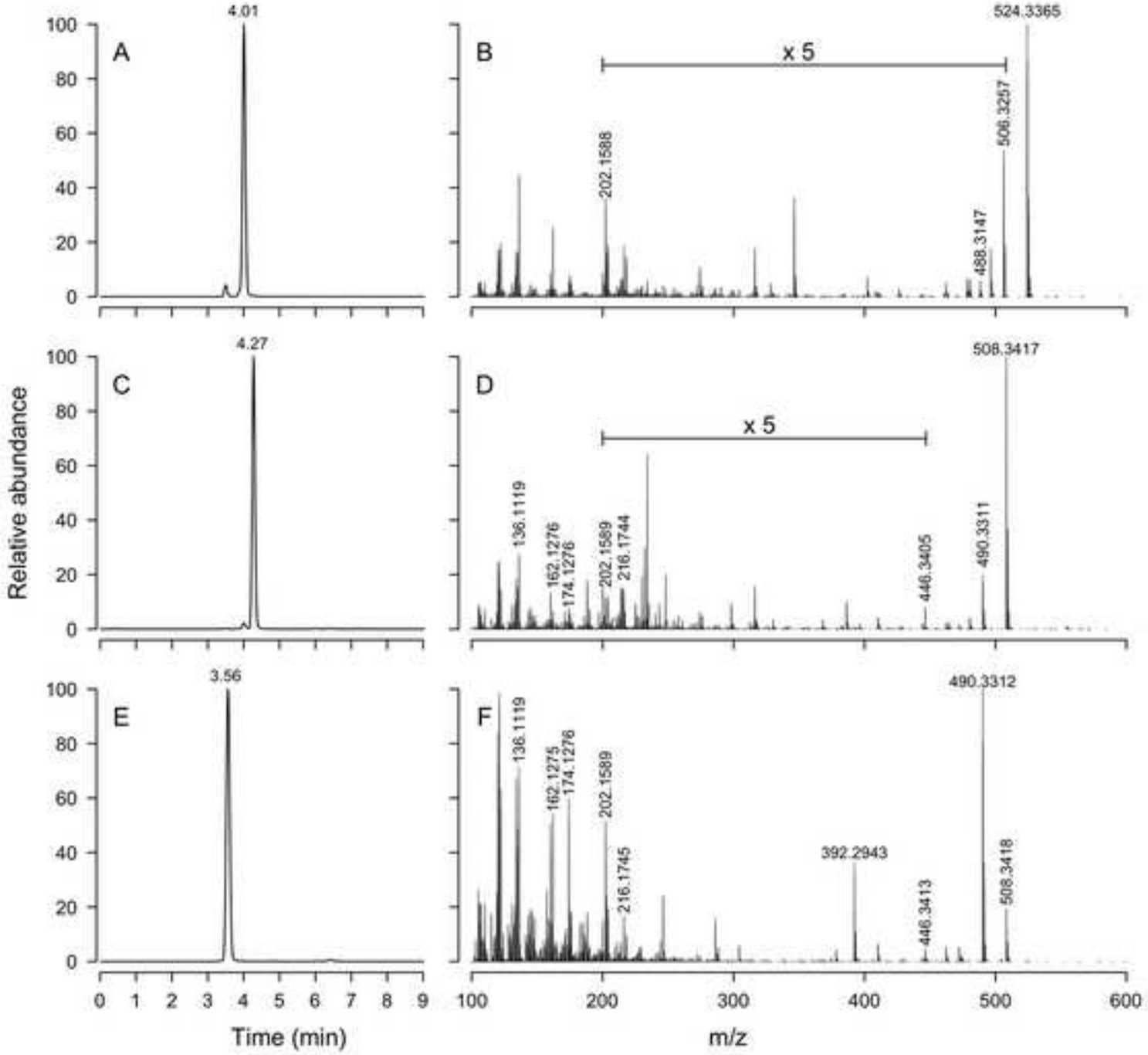

Figure

Click here to download high resolution image